

Chemistry–A European Journal

Supporting Information

Design, Synthesis and Aromaticity of an Alternating Cyclo[4]Thiophene[4]Furan

Manami Kawakami, Dhruv Sharma, Anthony J. Varni, Stephanie Tristram-Nagle, David Yaron,
Tomasz Kowalewski,* and Kevin J. T. Noonan*

Supporting Information

Table of Contents

Materials and Methods.....	S3-S6
Experimental Procedures	S7-S14
NMR spectra (Figures S1-S8).....	S15-S25
HRMS Spectra (Figures S9-S15).....	S26-S28
FT-IR Spectrum of C4TE4FE (Figure S16)	S29
Determination of Onset Potentials from CV (Figure S17)	S30
Experimental Procedure for $(\text{C4FE4TE})^{2+} \cdot 2(\text{SbCl}_6^-)$ and $(\text{C6FE})^{2+} \cdot 2(\text{SbCl}_6^-)$	S31
NMR spectra of $(\text{C4FE4TE})^{2+} \cdot 2(\text{SbCl}_6^-)$ and $(\text{C6FE})^{2+} \cdot 2(\text{SbCl}_6^-)$ (Figure S18-S20) ...	S32-S34
EPR spectra of $(\text{C4FE4TE})^{2+} \cdot 2(\text{SbCl}_6^-)$ (Figure S21)	S35
UV-Vis-NIR spectrum of isolated $(\text{C4FE4TE})^{2+} \cdot 2(\text{SbCl}_6^-)$ and $(\text{C6FE})^{2+} \cdot 2(\text{SbCl}_6^-)$ (Figure S22-23)	S36
Ring-strain energy calculations for C4TE4FE and C6FE (Figure S24-25)	S37
Bond alternation pathway and Mulliken charge distribution per ring calculations for a linear and cyclic alternating thiophene-furan oligomer. (Figure S26)	S38
NICS plots for methyl furan-3-carboxylate and methyl thiophene-3-carboxylate along with furan and thiophene (Figure S27).....	S39
Bar chart illustration of the NICS(1) _{zz} value for <i>me</i> -C6FE and <i>me</i> -C4TE4FE (Figure S28) ...	S40

ELF plots for neutral and dication macrocycles (Figure S29-S30)	S41-S42
LOL plots for C4TE4FE and C6FE (Figure S31-S32)	S43
TD-DFT plots for <i>me</i> -C4TE4FE – neutral, dication singlet, and dication triplet states (Figure S33)	S44
Shielding Tensors and Computed Chemical Shifts for <i>me</i> -C6FE and <i>me</i> -C4TE4FE (Table S1)	S45
References	S46

Materials and Methods. All reactions and manipulations of air and water sensitive compounds were carried out in a N₂ atmosphere using an mBraun glovebox or standard Schlenk techniques with dried and degassed solvents. All reagents were purchased from commercial sources and used as received. The dichloromethane used in the synthesis of [C₄TE₄FE]²⁺⁺• 2SbCl₆⁻ and attempted synthesis of [C₆FE]²⁺⁺• 2SbCl₆⁻ was spectrophotometric grade. All solvents and chemicals used for extraction and column chromatography were used as received. Flash chromatography was completed using a Biotage Isolera One Flash Chromatography System using Aldrich technical grade silica gel (pore size 60 Å, 70-230 mesh, 63-200 μm). Hexyl 2-bromofuran-3-carboxylate, hexyl 2-bromothiophene-3-carboxylate, hexyl 5-(4,4,5,5-tetramethyl-1,3,2-dioxaborolan-2-yl)furan-3-carboxylate were prepared according to literature procedures.^{[1],[2]} 2,2,6,6-Tetramethylpiperidinylmagnesium chloride lithium chloride complex solution is abbreviated as TMPMgCl·LiCl. (1,5-cyclooctadiene)(methoxy)iridium(I) dimer and 4,4'-di-*tert*-butyl-2,2'-dipyridyl are abbreviated as [Ir(COD)(OMe)]₂ and dtbpy, respectively. [1,3-bis(2,6-diisopropylphenyl)imidazol-2-ylidene](3-chloropyridyl)palladium(II) dichloride is abbreviated as PEPPSI-IPr.

NMR Analysis. All NMR experiments were collected at 300 K on a two-channel Bruker Avance III NMR instrument equipped with a Broad Band Inverse (BBI) probe, operating at 500 MHz for ¹H (126 MHz for ¹³C, 160 MHz for ¹¹B). The ¹H NMR spectra are referenced to CHCl₃ (7.26 ppm) and CD₂Cl₂ (5.32 ppm) and the ¹³C NMR spectra are referenced to CDCl₃ (77.2 ppm) and CD₂Cl₂ (54.0 ppm). ¹¹B spectra were referenced to the lock signal. In the ¹³C NMR spectra collected for borylated arenes, no signal is observed for the carbon atom directly attached to the boron due to quadrupolar relaxation.

Mass Spectrometry. DART-MS (positive mode, 150-300 °C) and ESI-MS measurements were performed on a Thermo Scientific Exactive Plus EMR Orbitrap Mass Spectrometer. Samples were prepared as 0.2 mg/mL solutions (in THF or methanol). In most cases $[M + NH_4]^+$ or $[M + H]^+$ species were observed along with dimer type adducts.

MALDI-TOF measurements were performed on a Bruker UltraFlex extreme MALDI-TOF-MS in linear mode with *trans*-2-[3-(4-tert-butylphenyl)-2-methyl-2-propenylidene]malononitrile (DCTB) as the matrix. A 10 mg/mL DCTB solution in $CHCl_3$ was drop-cast onto the target plate. Subsequently, a 20 mg/mL macrocycle solution in $CHCl_3$ was mixed with the matrix on the same target plate.

Cyclic Voltammetry. Electrochemical potentials were determined using a Bio-Logic SP-150 Potentiostat with a potential sweep rate of 100 mV/s. A 1 mm² glassy carbon working electrode, a platinum coil counter electrode, and a silver wire pseudo-reference electrode were employed for the measurements. The voltammogram was referenced using Fc/Fc⁺ as an internal standard [0.46 V (E_{Fc/Fc^+}) vs. SCE for CH_2Cl_2]. Tetra-*n*-butylammonium hexafluorophosphate served as the supporting electrolyte at a concentration of 0.01 M in CH_2Cl_2 . The CH_2Cl_2 solutions with the supporting electrolyte and analyte were degassed for 30 min with bubbling Ar prior measurement. A 0.63 mg/mL solution in CH_2Cl_2 was used for the measurements.

UV-Vis Spectroscopy. UV-Vis spectra of all compounds were recorded on a Varian Cary 5000 spectrophotometer. Prior to recording the spectra for all macrocycles, a 100% transmittance sample was taken of the cuvette (quartz, 10 mm × 10 mm). The “blank” of the solvent ($CHCl_3$ or CH_2Cl_2) was then collected for baseline subtraction during analysis. Solution measurements were completed using $CHCl_3$ or CH_2Cl_2 at concentrations of ~0.0075 mg/mL.

Infrared Spectroscopy. FTIR attenuated total reflectance spectroscopy was performed using a PerkinElmer Frontier FTIR spectrometer with a germanium crystal. Spectra were acquired with a 0.25 cm^{-1} resolution over a range of $700\text{-}4000\text{ cm}^{-1}$ and corrected for attenuated total reflectance.

Powder X-ray Diffraction. Powder X-ray diffraction data were collected using a Rigaku rotating anode RUH3R (The Woodlands, TX). Samples were prepared by loading powder into the tip of 1 mm float glass capillaries. These capillaries were then loaded into a custom holder such that the sample was in line with the beam. Cu K α radiation with $\lambda = 1.5418\text{ \AA}$ was used; beam size was $1.0 \times 1.0\text{ mm}$, focused with a Xenocs Fox2D focusing collimator and Huber slit. 2D images were collected on a Flicam CCD detector (Fingerlakes Instrumentation, Lima, NY) in 10 min dezingered scans. The sample-to-CCD distance was 105.9 mm, calibrated with silver behenate powder ($d = 58.367\text{ \AA}$).

EPR Spectroscopy. X-band CW EPR spectra were collected with a Bruker ELEXYS-II E500 EPR spectrometer equipped with an Oxford ESR-910 liquid helium cryostat. The signal was quantified relative to a previously prepared Cu(II)(EDTA) spin standard. The microwave frequency was calibrated with a frequency counter, while the magnetic field was calibrated with an NMR gaussmeter. Unless specifically specified, the following standard parameters were used for each EPR spectrum: 100 kHz modulation frequency, 1 G modulation amplitude, 150 ms conversion time, 9.63 GHz microwave frequency. Each sample was analyzed at an appropriate microwave power and sample temperature to satisfy non saturating conditions. EPR spectra were plotted and analyzed by using the software SpinCount.^[3]

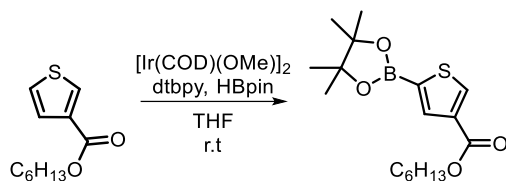
Computational Studies. Calculations were performed for the macrocycles with methyl ester side chains instead of the experimentally synthesized hexyl ester substituted macrocycles. Density functional theory (DFT) and time-dependent DFT (TD-DFT) calculations were performed using

Gaussian 16.^[4] Gas phase torsional potential energy scans and geometry optimizations were computed using B3LYP-D3(BJ) and ω B97XD functionals and 6-31G(d,p) basis sets. CAM-B3LYP/6-31G(d,p) was used for TD-DFT calculations. All calculations/optimizations except the torsional scans were completed using a Polarizable Continuum Model (PCM) with the integral equation formalism variant (IEFPCM) and CH₂Cl₂ as the solvent. Localized-orbital locator (LOL^[5]), and electron localization function (ELF^[6]) analyses were carried out using the Multiwfn^[7] package and Isosurface images were generated in Multiwfn or using custom routines written in Mathematica (Wolfram Research, Inc).

NICS calculations were performed using the Gauge-Independent Atomic Orbital (NMR-GIAO) method on a polar grid of points placed 1 angstrom above the plane of the macrocycle. The results were visualized using Mathematica with custom written routines.

Optimized geometries for all relevant structures are included as a compressed folder with relevant .xyz files. The naming scheme follows the form: (C)4T(E)4F(E)/C6F(E)_(q)S/T_(p) where C4T4F is cyclo[4]thiophene[4]furan macrocycle and C6F is cyclo[6]furan macrocycle, optional characters shown in parentheses indicate the molecule form (C – cyclic, L – linear), the side group (E - methyl ester, no label - unsubstituted), charges (q = N2 for dianion, P2 for dication, 0 for neutral, N1 for anion, and P1 for cation), functional (p= b for B3LYP-D3(BJ) and w for ω B97xD), and S or T refers to singlet or triplet state.

Experimental Procedures



hexyl 5-(4,4,5,5-tetramethyl-1,3,2-dioxaborolan-2-yl)thiophene-3-carboxylate.

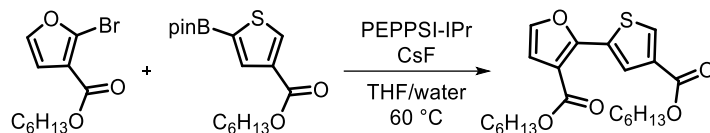
In a N₂ filled glovebox, a 20 mL scintillation vial was charged with [Ir(COD)(OMe)₂] (23 mg, 0.035 mmol), dtbpy (19 mg, 0.071 mmol), and 4 mL THF, and stirred for 30 min at room temperature. To this mixture, pinacolborane (1.1 mL, 7.6 mmol) was added, and the reaction mixture was stirred for additional 30 min. The reaction mixture went from light green-brown to dark red-brown during that period. Hexyl thiophene-3-carboxylate (1.50 g, 7.07 mmol) was then added dropwise (Caution: H₂ gas evolves in this step). An additional 10 mL THF was used to aid quantitative transfer of the compound to the reaction vial. The solution was kept in the glovebox and stirred overnight. Upon confirmation of borylation via crude ¹H NMR spectroscopy, the vial was removed from the glovebox. The reaction mixture was concentrated using rotary evaporation. The crude product was then purified by column chromatography (gradient from 1:0 to 1:2 of hexanes: CH₂Cl₂). The final product was collected as a colorless oil (2.02 g, 84%).

¹H NMR (500 MHz, CDCl₃) δ 8.33 (d, *J* = 1.0 Hz, 1H), 8.03 (d, *J* = 1.0 Hz, 1H), 4.26 (t, *J* = 6.7 Hz, 2H), 1.77 – 1.68 (m, 2H), 1.46 – 1.38 (m, 2H), 1.38 – 1.30 (m, 16H), 0.93 – 0.87 (m, 3H).

¹¹B-NMR (160 MHz, CDCl₃): δ 29.0.

¹³C NMR (126 MHz, CDCl₃) δ 162.9, 139.1, 138.0, 135.4, 84.6, 65.0, 31.6, 28.9, 25.8, 24.9, 22.7, 14.2

ESI-MS (*m/z*): [M+H]⁺ calculated for C₁₇H₂₈BO₄S, 339.1796; found, 339.1793.



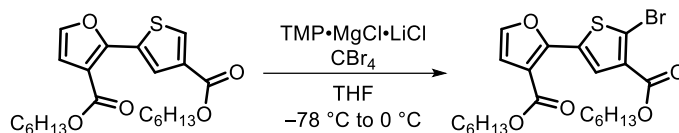
Hexyl 2-(4-((hexyloxy)carbonyl)thiophen-2-yl)furan-3-carboxylate (FETE).

In a N₂ filled glovebox, an oven-dried 125 mL Schlenk flask was charged with PEPPSI-IPr (48 mg, 0.07 mmol), CsF (1.07 g, 7.04 mmol), hexyl 2-bromofuran-3-carboxylate (0.97 g, 3.52 mmol), and hexyl 5-(4,4,5,5-tetramethyl-1,3,2-dioxaborolan-2-yl)thiophene-3-carboxylate (1.68 g, 4.96 mmol). Then, 35 mL of additional THF was added to the flask, which was sealed and removed from the glovebox. The flask was opened to N₂ on a Schlenk manifold and placed in a 60 °C oil bath. Then, 1.3 mL of degassed deionized water was added with a syringe. The reaction was stirred overnight, after which the flask was cooled to room temperature. The crude mixture was concentrated via rotary evaporation and transferred to a 500 mL separatory funnel. Approximately 200 mL of H₂O was added, and the aqueous layer was extracted with diethyl ether (3 × 100 mL). The combined organic extracts were washed with water and brine, dried using Na₂SO₄, and concentrated using rotary evaporation. The crude product was then purified by column chromatography (gradient from 1:0 to 1:2 of hexanes:CH₂Cl₂). The final product was collected as a viscous, slightly yellow oil (1.30 g, 91%).

¹H NMR (500 MHz, CDCl₃) δ 8.31 (d, *J* = 1.4 Hz, 1H), 8.14 (d, *J* = 1.4 Hz, 1H), 7.37 (d, *J* = 1.9 Hz, 1H), 6.81 (d, *J* = 1.9 Hz, 1H), 4.30 (t, *J* = 6.8 Hz, 2H), 4.28 (t, *J* = 6.8 Hz, 2H), 1.79 – 1.71 (m, 4H), 1.47 – 1.37 (m, 4H), 1.37 – 1.28 (m, 8H), 0.95 – 0.86 (m, 6H).

¹³C NMR (126 MHz, CDCl₃) δ 163.4, 162.8, 152.0, 141.2, 134.3, 134.1, 132.3, 128.9, 113.5, 112.9, 65.21, 65.17, 31.7, 31.6, 28.9, 28.8, 25.9, 25.8, 22.74, 22.73, 14.19, 14.18.

ESI-MS (*m/z*): [M+H]⁺ calculated for C₂₂H₃₁O₅S, 407.1887; found, 407.1885.



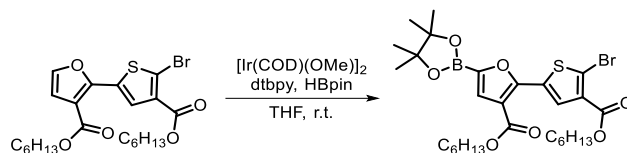
hexyl 2-(5-bromo-4-((hexyloxy)carbonyl)thiophen-2-yl)furan-3-carboxylate (FETE-Br).

An oven-dried 125 mL Schlenk flask was charged with hexyl 2-(4-((hexyloxy)carbonyl)thiophen-2-yl)furan-3-carboxylate (2.13 g, 5.24 mmol) under N₂. Then, 52 mL of dry THF was added to the flask, and the solution was cooled to -78 °C using a dry-ice acetone bath. A 1 M TMPMgCl·LiCl in THF/toluene (5.8 mL, 5.8 mmol) was added to the solution by syringe over a 10 min period. The reaction mixture was stirred for 1.5 h at -78 °C, then CBr₄ (1.91 g, 5.76 mmol) in 10 mL dry THF was added dropwise by syringe over 5 min. The reaction mixture was warmed to 0 °C and stirred for 1 h. Then, a 1 M HCl solution (10 mL) was used to quench the reaction mixture. The reaction mixture was concentrated, and the remaining solution was transferred to a 500 mL separatory funnel, diluted with 200 mL of deionized H₂O and extracted with diethyl ether (3 × 100 mL). The combined organic extracts were washed with water and brine, dried using Na₂SO₄, and concentrated using rotary evaporation. The crude product was purified by column chromatography (gradient from 1:0 to 1:1 of hexanes:CH₂Cl₂). The final product was collected as a yellow oil (2.16 g, 85%).

¹H NMR (500 MHz, CDCl₃) δ 8.10 (s, 1H), 7.37 (d, *J* = 1.9 Hz, 1H), 6.79 (d, *J* = 1.9 Hz, 1H), 4.33 – 4.27 (m, 4H), 1.80 – 1.70 (m, 4H), 1.50 – 1.38 (m, 4H), 1.37 – 1.28 (m, 8H), 0.94 – 0.85 (m, 6H).

¹³C NMR (126 MHz, CDCl₃) δ 163.5, 162.0, 151.3, 141.5, 131.4, 131.3, 129.5, 122.6, 113.7, 112.7, 65.5, 65.3, 31.63, 31.61, 28.80, 28.78, 25.9, 25.8, 22.7, 14.20, 14.18. The signal at 22.7 corresponds to two overlapping signals from the alkyl chains.

ESI-MS (*m/z*): [M+H]⁺ calculated for C₂₂H₃₀BrO₅S, 485.0992; found, 485.0991.



hexyl 2-(5-bromo-4-((hexyloxy)carbonyl)thiophen-2-yl)-5-(4,4,5,5-tetramethyl-1,3,2-dioxaborolan-2-yl)furan-3-carboxylate (Bpin-FETE-Br)

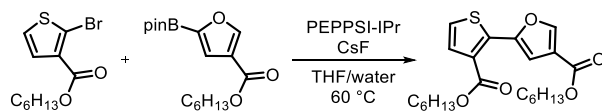
In a N₂ filled glovebox, a 20 mL scintillation vial was charged with [Ir(COD)(OMe)₂] (118 mg, 0.18 mmol), dtbpy (96 mg, 0.36 mmol) and 2 mL THF, then the mixture was stirred for 30 min at room temperature. Pinacolborane (3.8 mL, 26.2 mmol) was added to the solution, and the mixture was stirred for additional 30 min. The reaction went from light green-brown to dark red-brown during that period. Finally, hexyl 2-(5-bromo-4-((hexyloxy)carbonyl)thiophen-2-yl)furan-3-carboxylate (4.30 g, 8.86 mmol) was added dropwise (Caution: H₂ gas evolves in this step). An additional 2 mL THF was used to aid in quantitative transfer of the compound to the reaction flask. The solution was kept in the glovebox and stirred overnight. Borylation was confirmed by crude ¹H NMR spectroscopy after which, the vial was removed from the glovebox. The reaction mixture was concentrated using rotary evaporation and the crude product was purified by column chromatography (gradient from 1:0 to 1:1 of hexanes: CH₂Cl₂). The final product was collected as a yellow solid (3.46 g, 64%).

¹H NMR (500 MHz, CDCl₃) δ 8.24 (s, 1H), 7.42 (s, 1H), 4.31 (t, *J* = 6.7 Hz, 2H), 4.27 (t, *J* = 6.7 Hz, 2H), 1.82 – 1.69 (m, 4H), 1.51 – 1.29 (m, 24H), 0.95 – 0.87 (m, 6H).

¹¹B-NMR (160 MHz, CDCl₃): δ 28.1.

¹³C NMR (126 MHz, CDCl₃) δ 163.5, 162.1, 155.0, 131.4, 131.3, 130.6, 125.9, 123.3, 114.2, 84.9, 65.6, 65.3, 31.7, 31.6, 28.82, 28.81, 25.90, 25.88, 24.9, 22.7, 14.2. The signals at 22.7 and 14.2 each correspond to two overlapping signals from the alkyl chains.

ESI-MS (*m/z*): [M+H]⁺ calculated for C₂₈H₄₁BBrO₇S, 611.1844; found, 611.1849.



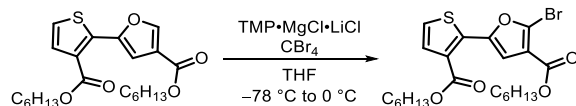
Hexyl 2-(4-((hexyloxy)carbonyl)furan-2-yl)thiophene-3-carboxylate (TEFE).

In a N₂ filled glovebox, an oven-dried 125 mL Schlenk flask was charged with PEPPSI-IPr (116 mg, 0.17 mmol), CsF (2.60 g, 17.1 mmol), hexyl 2-bromothiophene-3-carboxylate (2.50 g, 8.58 mmol), and hexyl 5-(4,4,5,5-tetramethyl-1,3,2-dioxaborolan-2-yl)furan-3-carboxylate (2.92 g, 9.06 mmol) along with 60 mL of THF. The flask was sealed, removed from the glovebox, and opened to N₂ on a Schlenk manifold. The flask was then placed in a 60 °C oil bath and 3.1 mL of degassed DI water was added with a syringe. The reaction was stirred overnight, after which the flask was cooled to room temperature. The crude mixture was concentrated via rotary evaporation and transferred to a 500 mL separatory funnel. Then, 200 mL of H₂O was added, and the aqueous layer was extracted with diethyl ether (3 × 100 mL). The combined organic extracts were washed with water and brine, dried using Na₂SO₄, and concentrated using rotary evaporation. The crude product was purified by column chromatography (gradient from 1:0 to 2:1 of hexanes:CH₂Cl₂). The final product was collected as a viscous, slightly yellow oil (3.42 g, 98%).

¹H NMR (500 MHz, CDCl₃) δ 8.01 (d, *J* = 0.7 Hz, 1H), 7.58 (d, *J* = 0.7 Hz, 1H), 7.50 (d, *J* = 5.4 Hz, 1H), 7.24 (d, *J* = 5.4 Hz, 1H), 4.28 (t, *J* = 6.8 Hz, 2H), 4.26 (t, *J* = 6.8 Hz, 2H), 1.77 – 1.69 (m, 4H), 1.45 – 1.37 (m, 4H), 1.37 – 1.28 (m, 8H), 0.93 – 0.86 (m, 6H).

¹³C NMR (126 MHz, CDCl₃) δ 163.03, 163.00, 148.6, 147.3, 138.2, 130.6, 127.9, 124.4, 121.9, 111.3, 65.3, 65.0, 31.6, 28.9, 28.8, 25.9, 25.8, 22.7, 14.2. The signals at 31.6, 22.7 and 14.2 each correspond to two overlapping signals from the alkyl chains.

DART-MS (*m/z*): [M+NH₄]⁺ calculated for C₂₂H₃₄NO₅S, 424.2152; found, 424.2136.



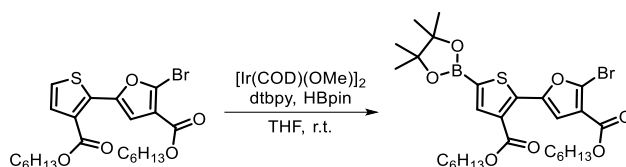
hexyl 2-(5-bromo-4-((hexyloxy)carbonyl)furan-2-yl)thiophene-3-carboxylate (TEFE-Br)

An oven-dried Schlenk flask under N_2 was charged with hexyl 5-(3-((hexyloxy)carbonyl)thiophen-2-yl)furan-3-carboxylate (1.16 g, 2.9 mmol) and 30 mL of dry THF. The solution was cooled to $-78\text{ }^\circ\text{C}$ using a dry-ice acetone bath and 1 M $\text{TMPMgCl}\cdot\text{LiCl}$ in THF/toluene (3.6 mL, 3.6 mmol) was added to the solution dropwise by syringe over 10 min. The reaction mixture was stirred for 1.5 h at $-78\text{ }^\circ\text{C}$, then CBr_4 (1.49 g, 4.5 mmol) in 10 mL dry THF was added dropwise with a syringe over 10 min. The reaction mixture was warmed to $0\text{ }^\circ\text{C}$ and stirred for 1 h. Then, a 1 M HCl solution (10 mL) was added to quench the reaction mixture and the mixture was concentrated. The remaining solution was transferred to a separatory funnel, diluted with 200 mL of deionized H_2O , and extracted with diethyl ether ($3 \times 100\text{ mL}$). The combined organic extracts were washed with water and brine, dried using Na_2SO_4 , and concentrated. The crude product was purified by column chromatography (gradient from 1:0 to 1:3 of hexanes: CH_2Cl_2). The final product was collected as an orange solid (0.80 g, 58%).

^1H NMR (500 MHz, CDCl_3) δ 7.58 (s, 1H), 7.50 (d, $J = 5.3\text{ Hz}$, 1H), 7.26 (d, $J = 5.3\text{ Hz}$, 1H), 4.28 (t, $J = 6.8\text{ Hz}$, 2H), 4.27 (t, $J = 6.8\text{ Hz}$, 2H), 1.78 – 1.68 (m, 4H), 1.48 – 1.36 (m, 4H), 1.36 – 1.28 (m, 8H), 0.95 – 0.84 (m, 6H).

^{13}C NMR (126 MHz, CDCl_3) δ 162.8, 161.9, 149.4, 137.0, 130.7, 128.9, 128.2, 124.8, 119.9, 113.9, 65.4, 65.3, 31.62, 31.60, 28.77, 28.76, 25.9, 25.8, 22.7, 14.2. The signals at 22.7 and 14.2 each correspond to two overlapping signals from the alkyl chains.

ESI-MS (m/z): $[\text{M}+\text{H}]^+$ calculated for $\text{C}_{22}\text{H}_{30}\text{BrO}_5\text{S}$, 485.0992; found, 485.0989.



hexyl 2-bromo-5-(3-((hexyloxy)carbonyl)-5-(4,4,5,5-tetramethyl-1,3,2-dioxaborolan-2-yl)thiophen-2-yl)furan-3-carboxylate (Bpin-TEFE-Br)

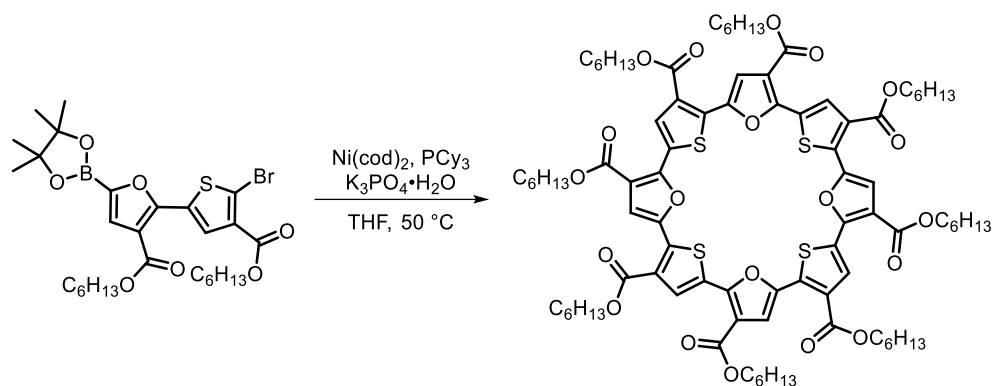
In a N₂ filled glovebox, a 20 mL scintillation vial was charged with [Ir(COD)OMe]₂ (34 mg, 0.05 mmol), dtbpy (28 mg, 0.10 mmol) and 2 mL THF, then stirred for 30 min at room temperature. Pinacolborane (0.56 mL, 3.9 mmol) was then added, and the mixture was stirred for 30 more min. The reaction turned dark red-brown. Hexyl 2-(5-bromo-4-((hexyloxy)carbonyl)furan-2-yl)thiophene-3-carboxylate (1.25 g, 2.58 mmol) was then added dropwise (Caution: H₂ gas evolves in this step) with some additional THF (2 mL) to aid quantitative transfer. The solution was kept in the glovebox and stirred overnight. The vial was then removed from the glovebox and the reaction mixture was concentrated. The crude product was purified by column chromatography (gradient from 1:0 to 1:3 of hexanes:CH₂Cl₂) and the final product was collected as a yellow solid (1.16 g, 74%).

¹H NMR (500 MHz, CDCl₃) δ 7.98 (s, 1H), 7.69 (s, 1H), 4.28 (t, *J* = 6.7 Hz, 2H), 4.27 (t, *J* = 6.7 Hz, 2H), 1.77 – 1.69 (m, 4H), 1.47 – 1.28 (m, 24H), 0.93 – 0.87 (m, 6H).

¹¹B-NMR (160 MHz, CDCl₃): δ 29.9.

¹³C NMR (126 MHz, CDCl₃) δ 162.9, 161.9, 149.7, 142.7, 140.3, 129.4, 128.8, 120.0, 114.4, 84.9, 65.4, 65.3, 31.7, 31.6, 28.83, 28.77, 25.9, 25.8, 24.9, 22.7, 14.21, 14.20. The signal at 22.7 corresponds to two overlapping signals from the alkyl chains.

ESI-MS (*m/z*): [M+H]⁺ calculated for C₂₈H₄₁BBrO₇S, 611.1844; found, 611.1843.



Representative Macrocyclization Procedure for C4TE4FE.

In a N₂ filled glovebox, a 20 mL scintillation vial was charged with 0.035 mmol of catalyst, K₃PO₄·H₂O (161 mg, 0.70 mmol), and monomer (214 mg, 0.35 mmol), and THF (11 mL). The vial was sealed, removed from the glovebox and 0.38 mL of degassed deionized water was added, then the mixture was heated for 24 h at 50 °C. The reaction mixture was then concentrated by rotary evaporation, and methanol was added to precipitate the macrocycle and polymer products. The crude product was isolated from residual small molecule byproducts by vacuum filtration, and then purified by column chromatography (1:0 to 1:2 of hexanes:CH₂Cl₂). The final product was collected as a brown solid.

¹H NMR (500 MHz, CDCl₃) δ 8.72 (s, 4H), 7.89 (s, 4H), 4.30 (t, *J* = 6.7 Hz, 8H), 4.28 (t, *J* = 7.0 Hz, 8H), 1.83 – 1.73 (m, 16H), 1.52 – 1.40 (m, 16H), 1.40 – 1.30 (m, 32H), 0.96 – 0.87 (m, 24H).

¹³C NMR (126 MHz, CDCl₃) δ 162.7, 162.6, 151.4, 146.2, 138.7, 134.3, 128.9, 128.2, 117.4, 117.0, 65.4, 65.2, 31.8, 31.7, 28.9, 28.8, 25.9, 25.8, 22.80, 22.77, 14.23, 14.19.

MALDI-TOF MS (*m/z*): [M]⁺ calculated for C₈₈H₁₁₂O₂₀S₄, 1616.663; found, 1616.707.

NMR Spectra

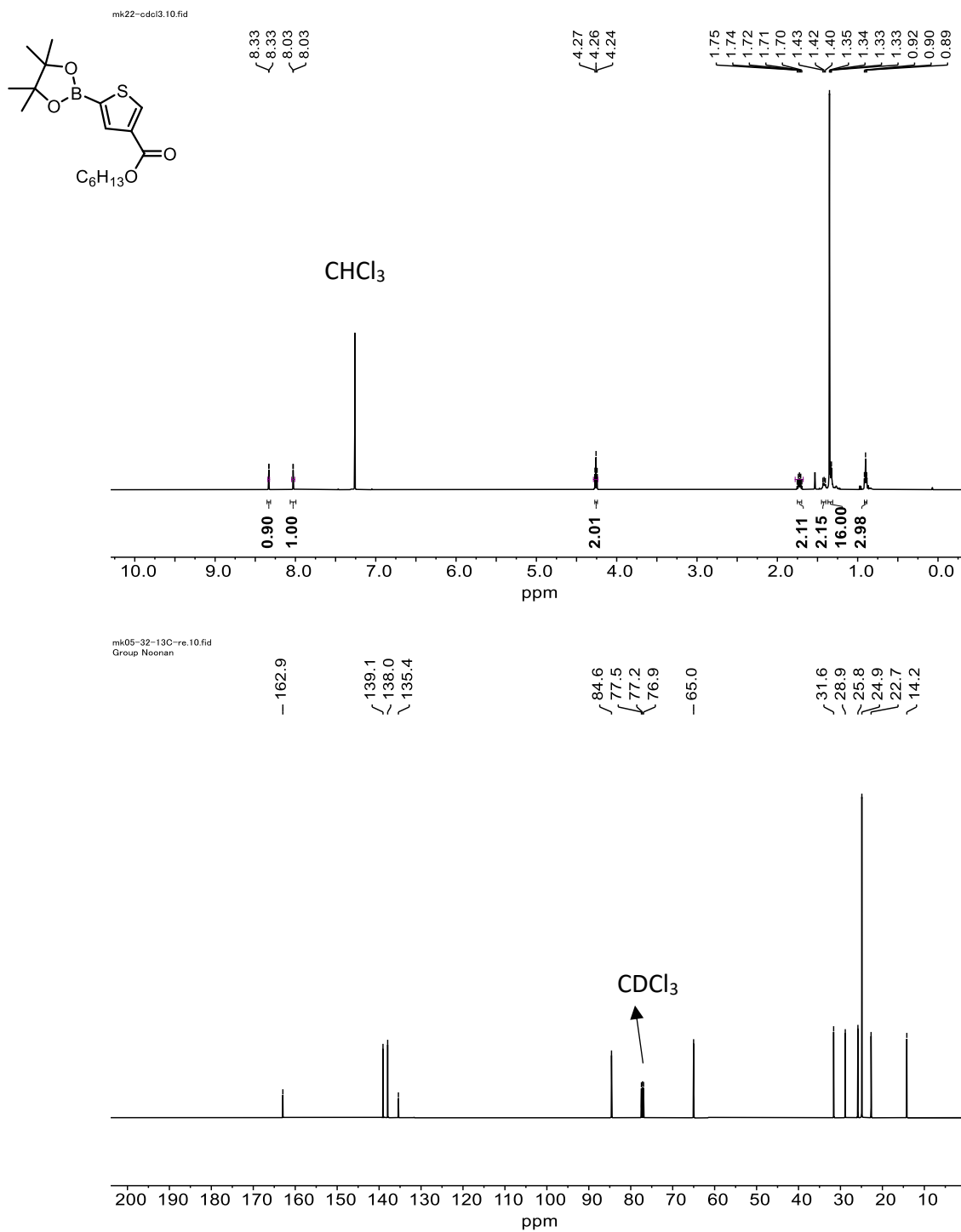


Figure S1a. ¹H (top) and ¹³C (bottom) NMR spectra of **hexyl 5-(4,4,5,5-tetramethyl-1,3,2-dioxaborolan-2-yl)thiophene-3-carboxylate** collected in CDCl₃ (500 and 126 MHz, respectively).

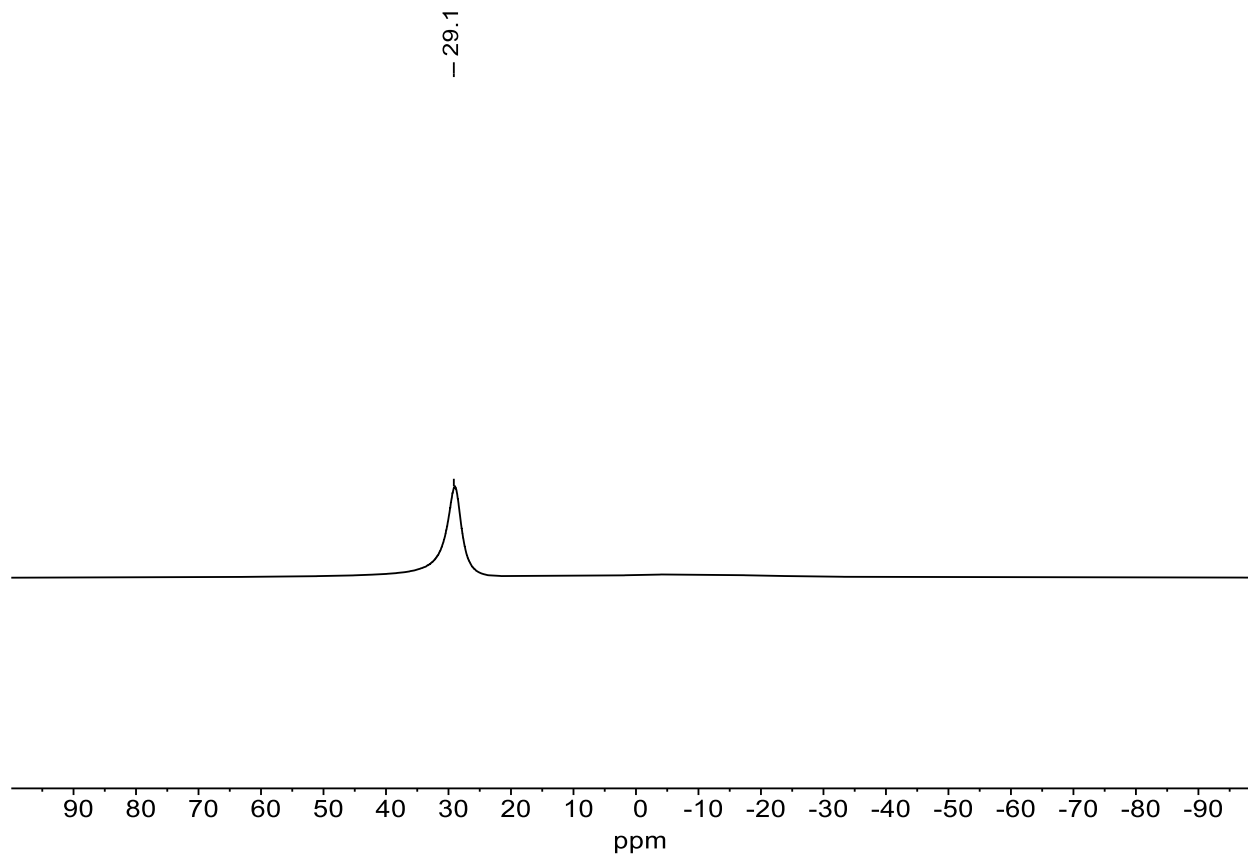


Figure S1b. $^{11}\text{B}\{^1\text{H}\}$ NMR spectrum (160 MHz, CDCl_3) of **hexyl 5-(4,4,5,5-tetramethyl-1,3,2-dioxaborolan-2-yl)thiophene-3-carboxylate** collected in CDCl_3 at room temperature.

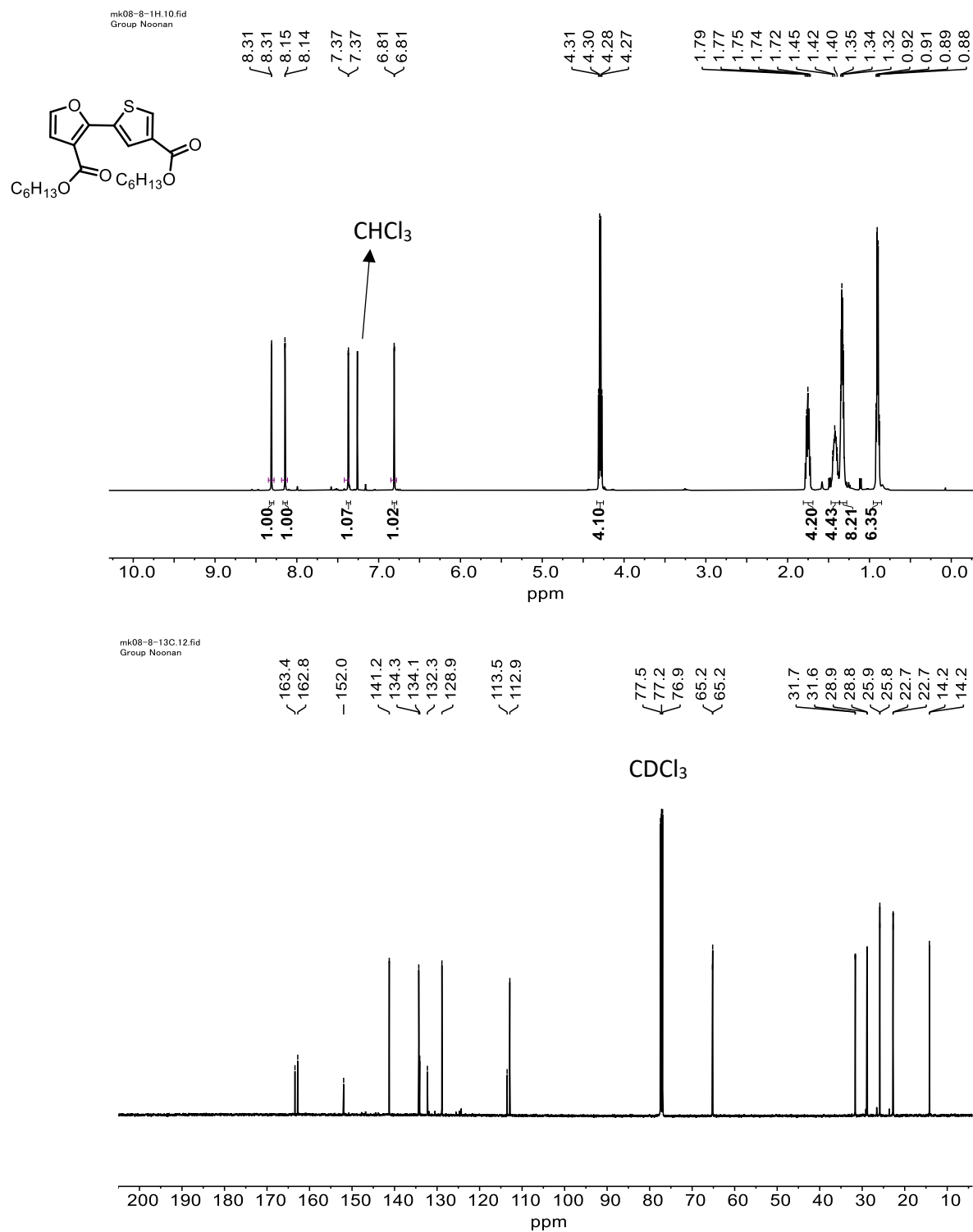


Figure S2. ¹H (top) and ¹³C (bottom) NMR spectra of **FETE** collected in CDCl₃ at room temperature (500 and 126 MHz, respectively).

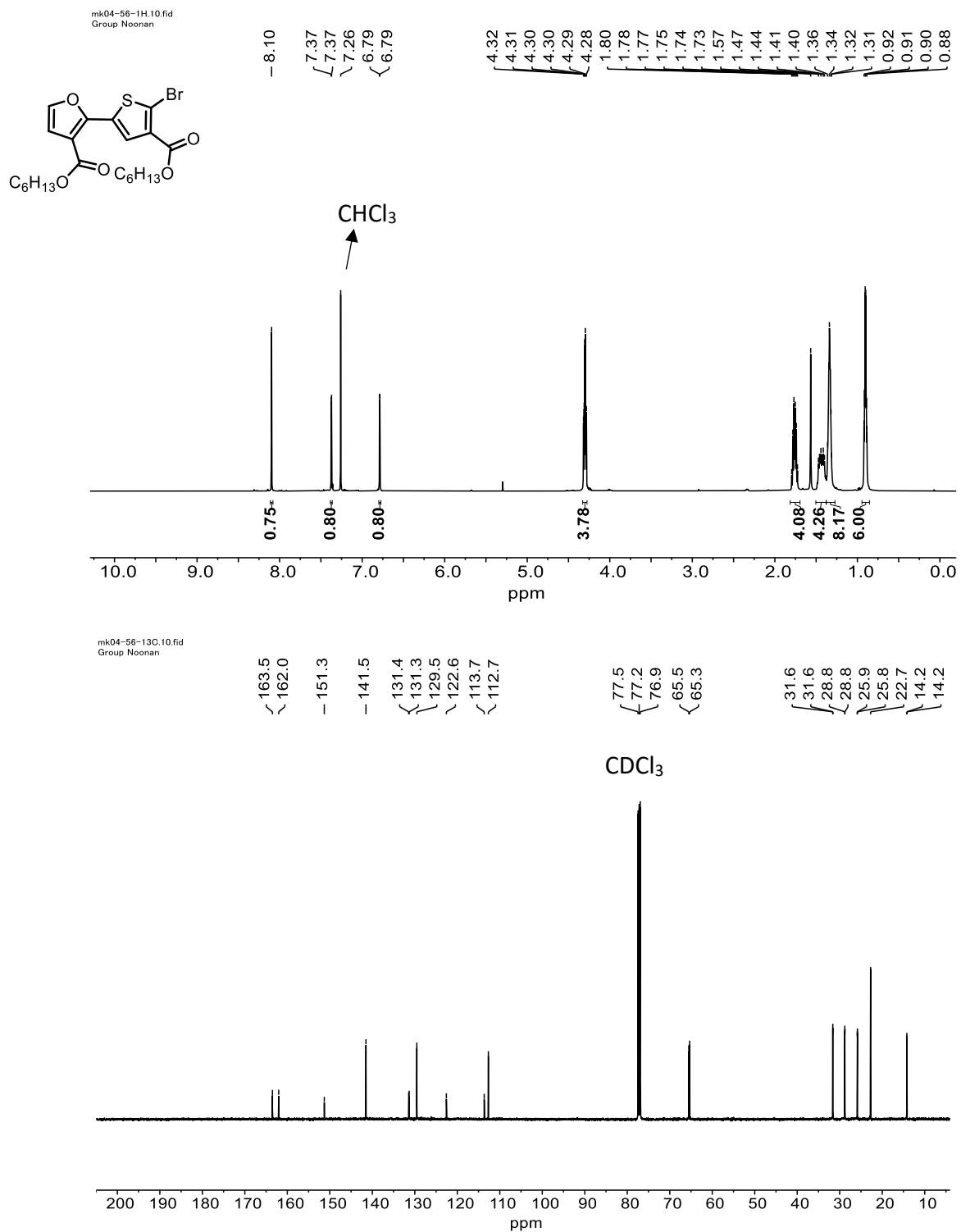


Figure S3. ¹H (top) and ¹³C (bottom) NMR spectra of **FETE-Br** collected in CDCl₃ at room temperature (500 and 126 MHz, respectively).

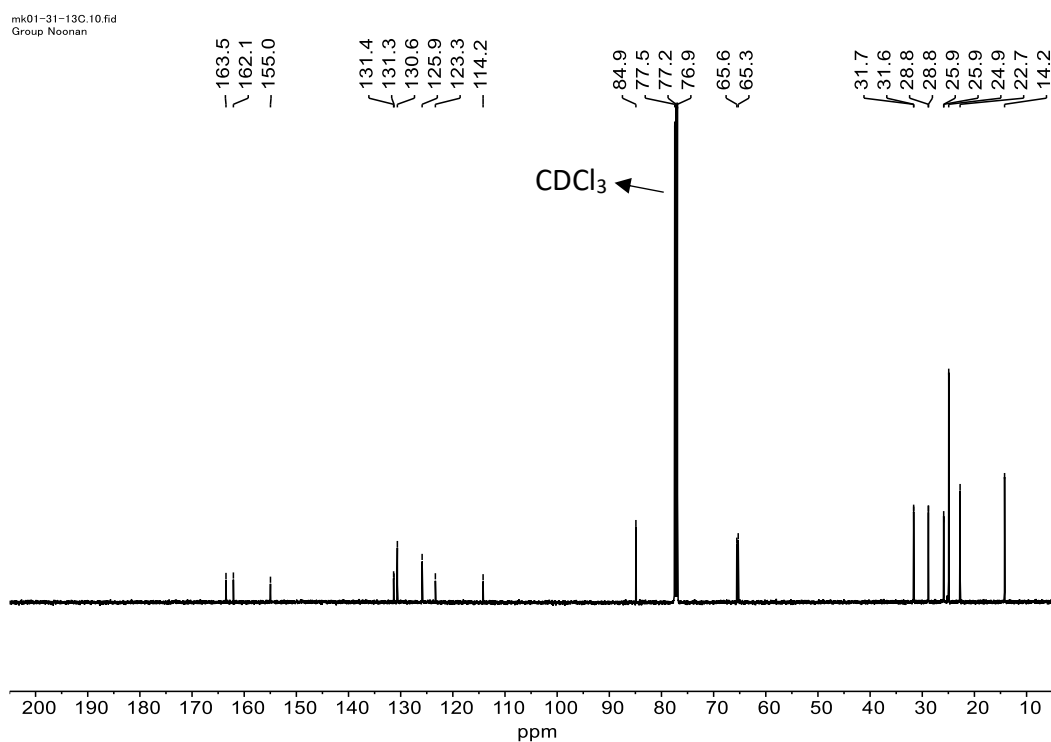
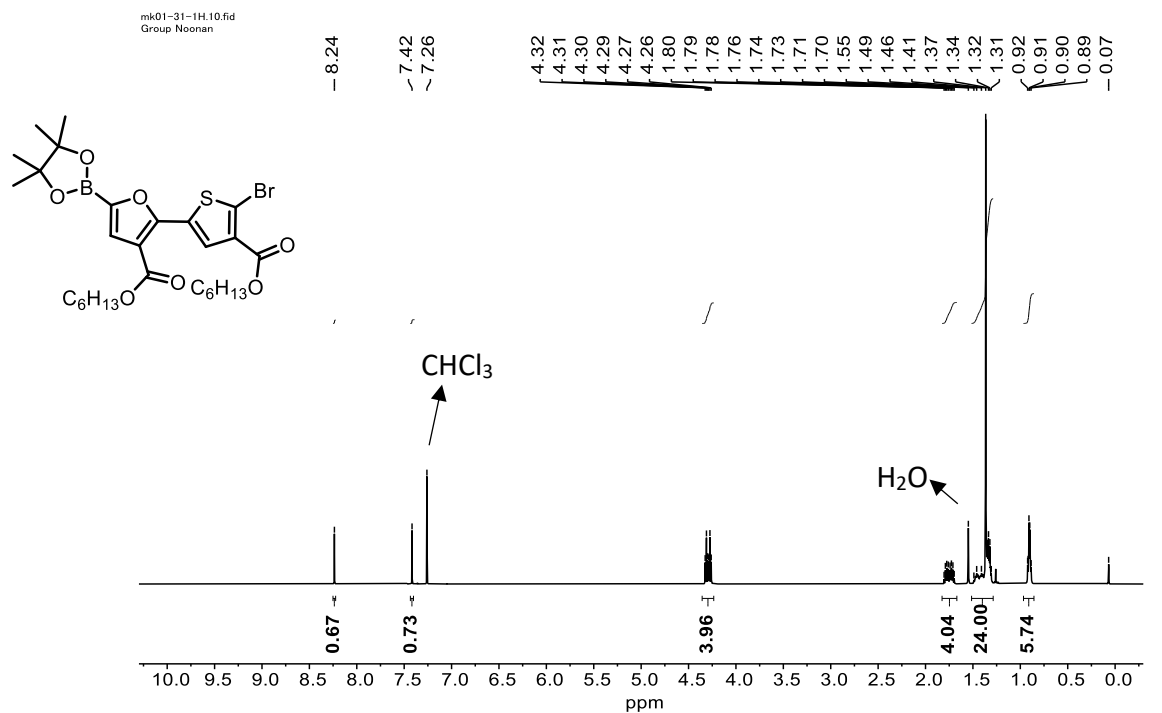


Figure S4a. ¹H (top) and ¹³C (bottom) NMR spectra of **Bpin-FETE-Br** collected in CDCl₃ at room temperature (500 and 126 MHz, respectively).

mk07-80-fr2-11B.10.fid

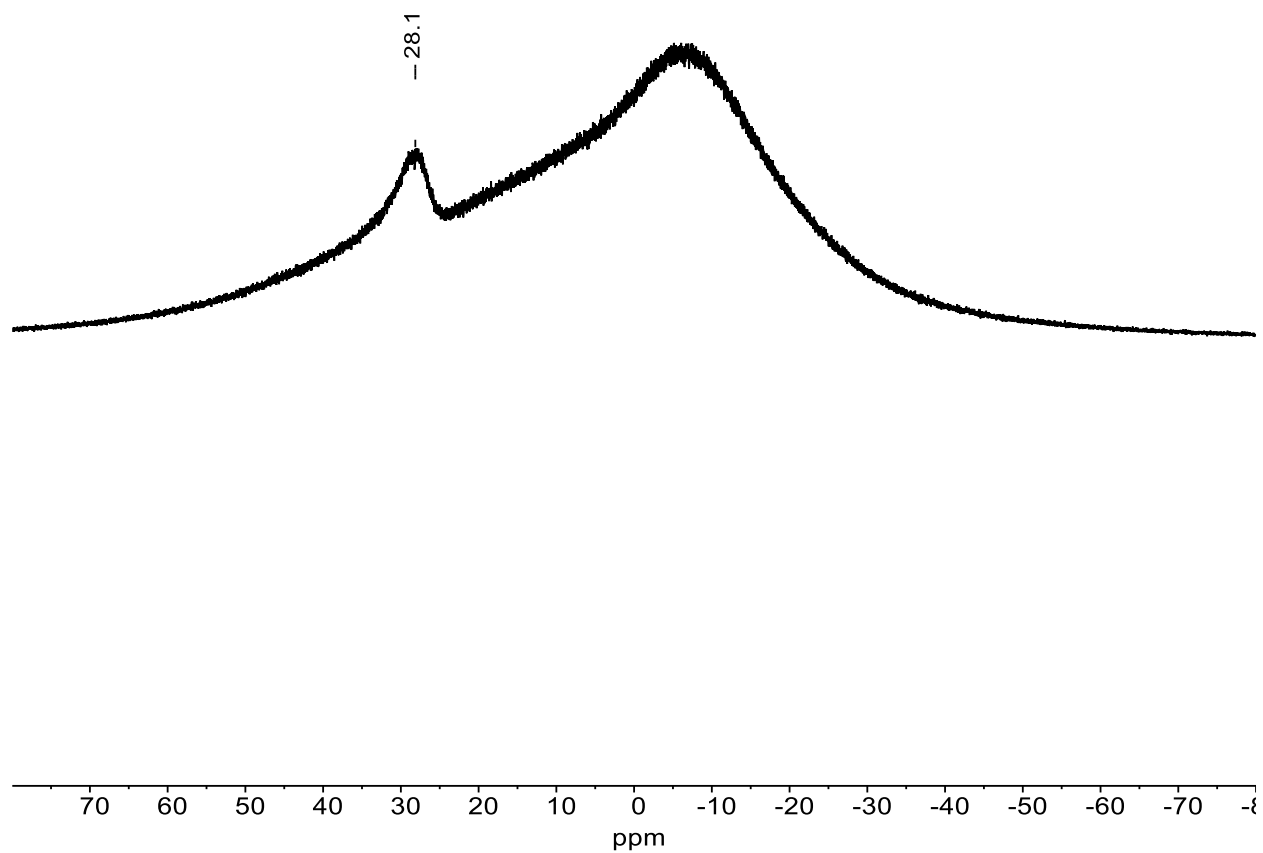


Figure S4b. $^{11}\text{B}\{^1\text{H}\}$ NMR spectrum (160 MHz, CDCl_3) of **Bpin-FETE-Br** collected in CDCl_3 at room temperature.

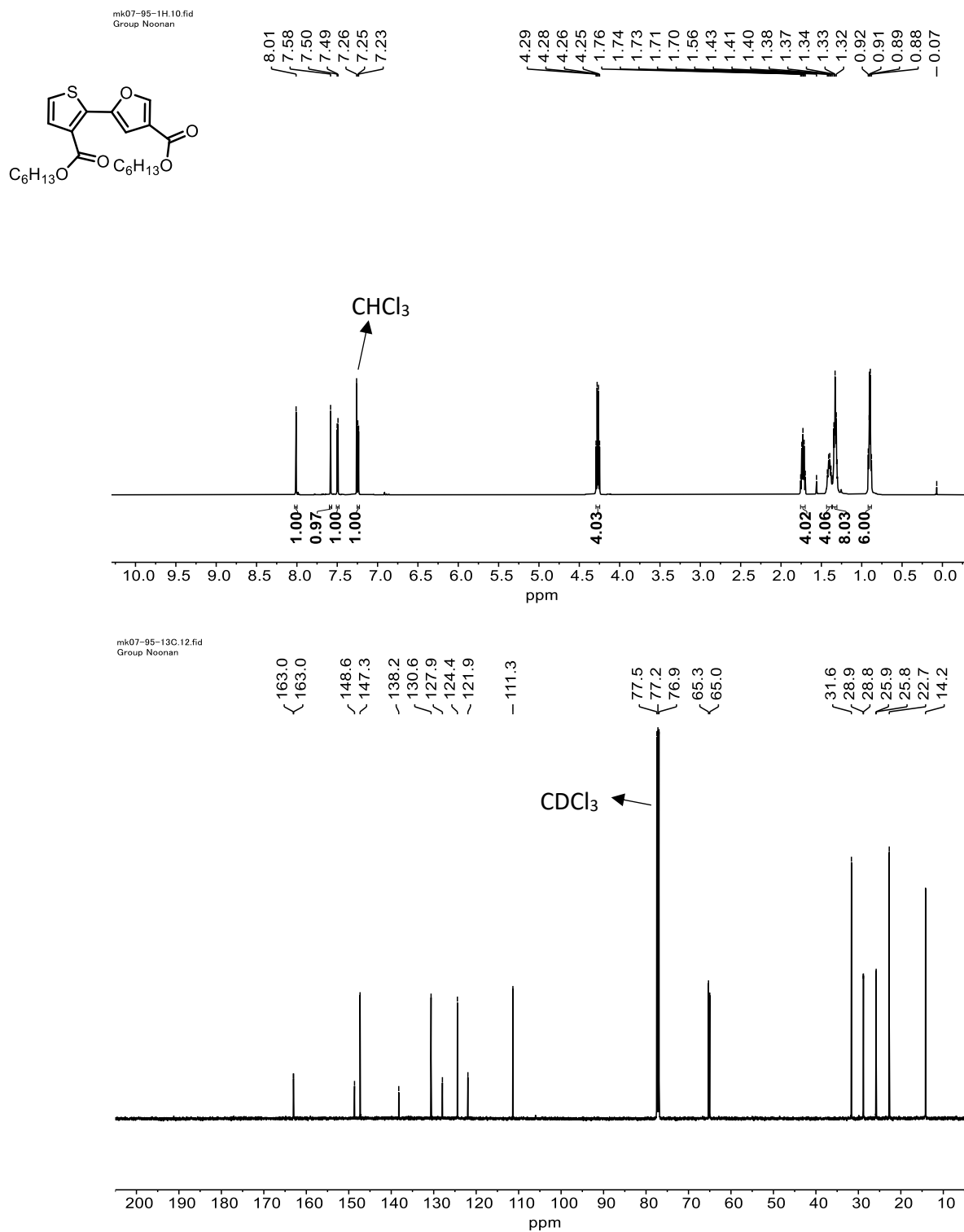


Figure S5. ¹H (top) and ¹³C (bottom) NMR spectra **TEFE** collected in CDCl₃ at room temperature (500 and 126 MHz, respectively).

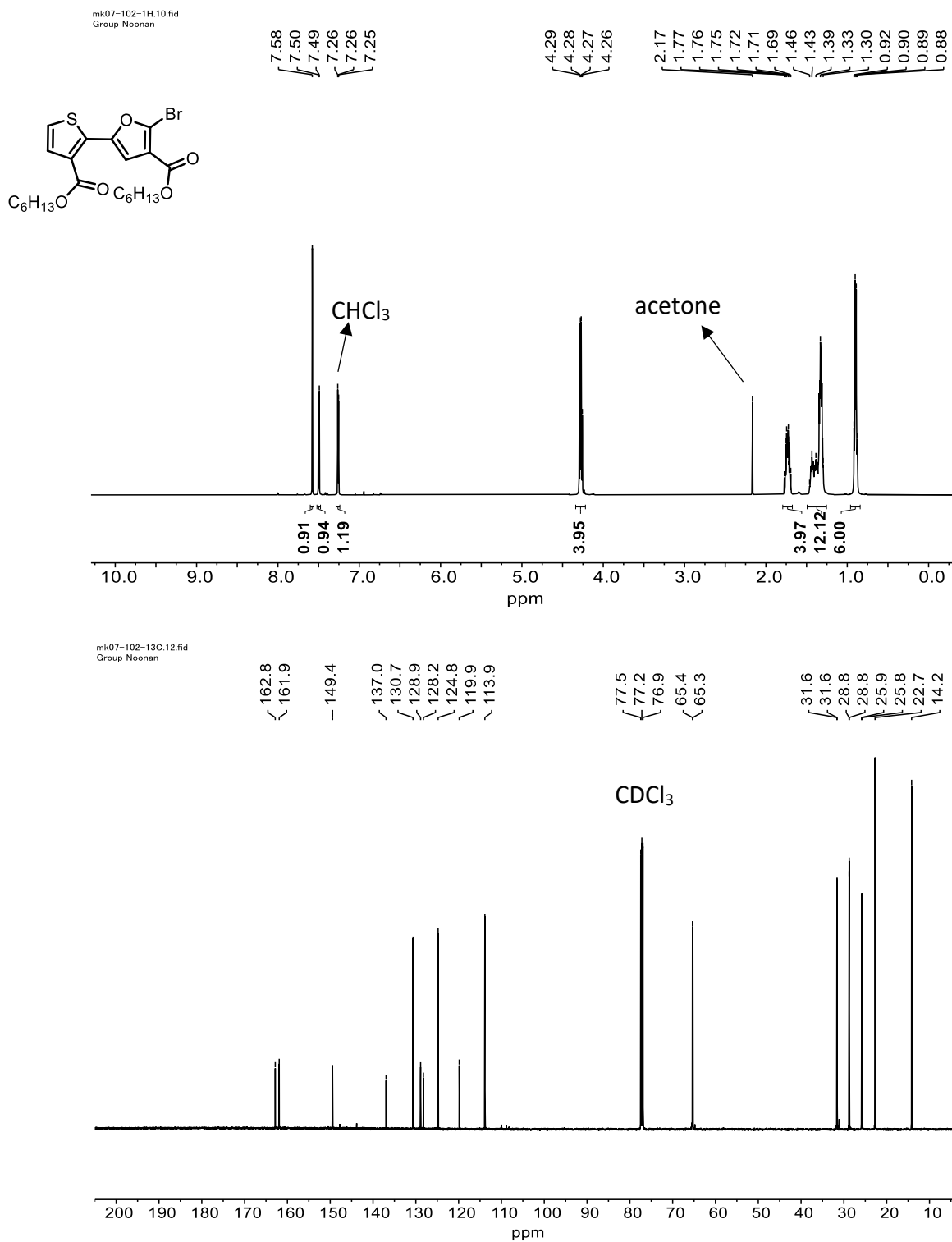


Figure S6. ¹H (top) and ¹³C (bottom) NMR spectra **TEFE-Br** collected in CDCl₃ at room temperature (500 and 126 MHz, respectively).

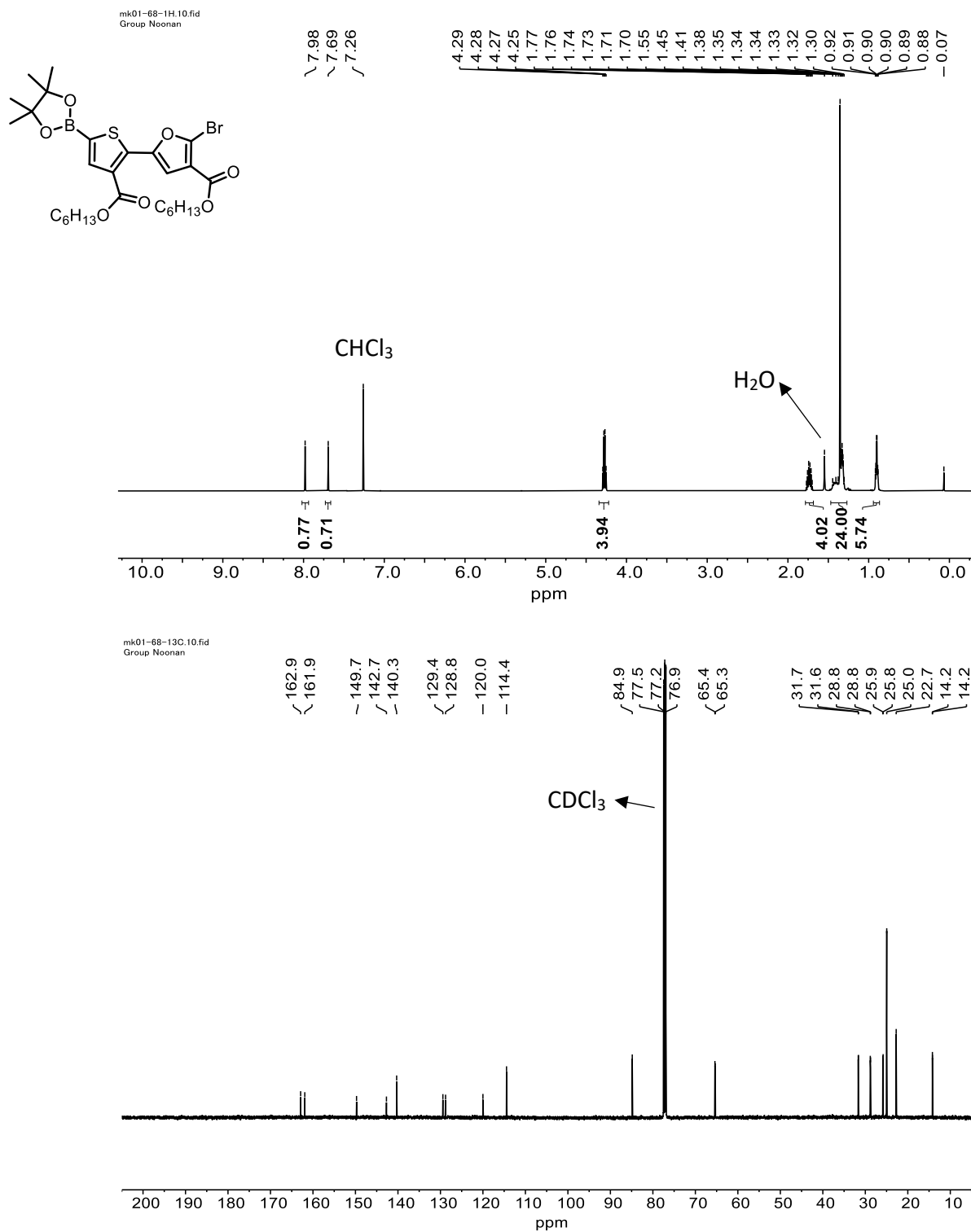


Figure S7a. ¹H (top) and ¹³C (bottom) NMR spectra **Bpin-TEFE-Br** collected in CDCl₃ at room temperature (500 and 126 MHz, respectively).

mk08-5-11B.10.fid

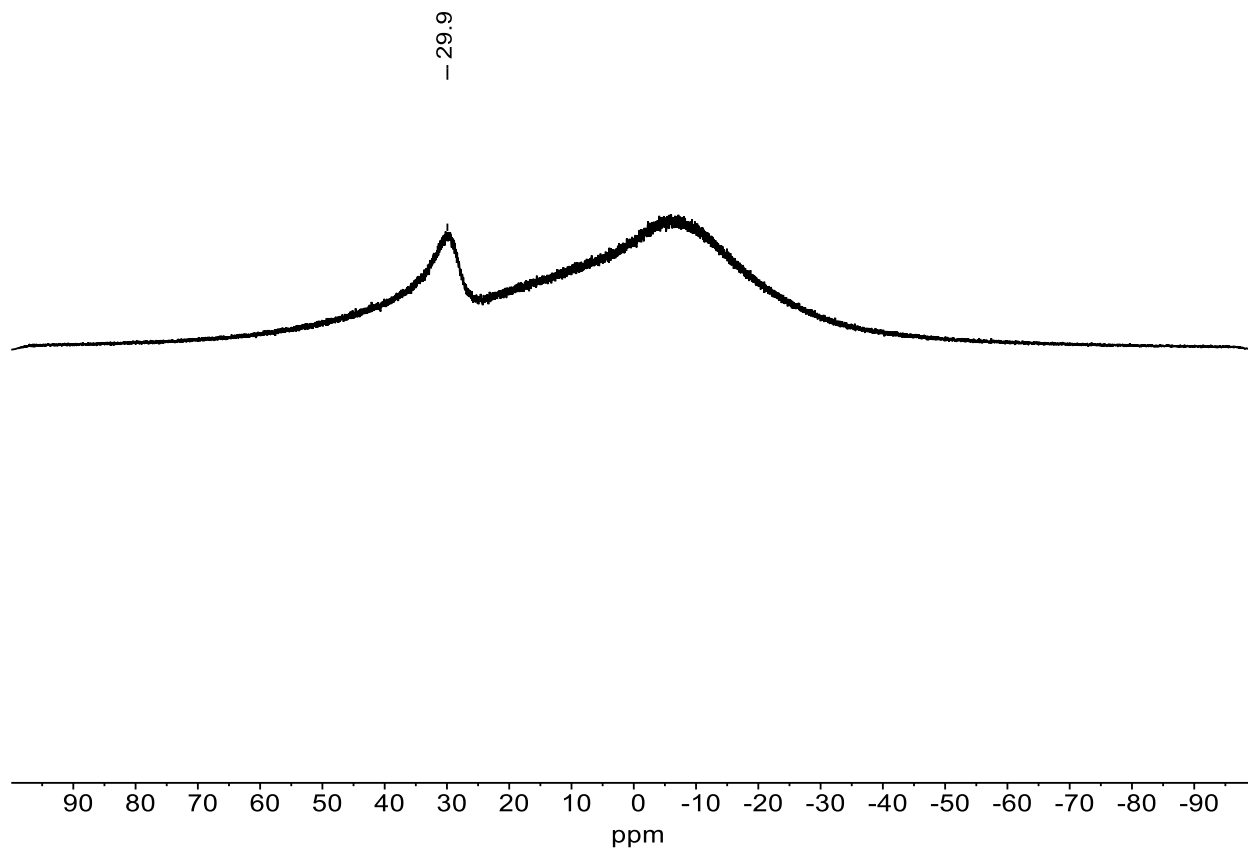


Figure S7b. $^{11}\text{B}\{^1\text{H}\}$ NMR spectrum (160 MHz, CDCl_3) of **Bpin-TEFE-Br** collected in CDCl_3 at room temperature.

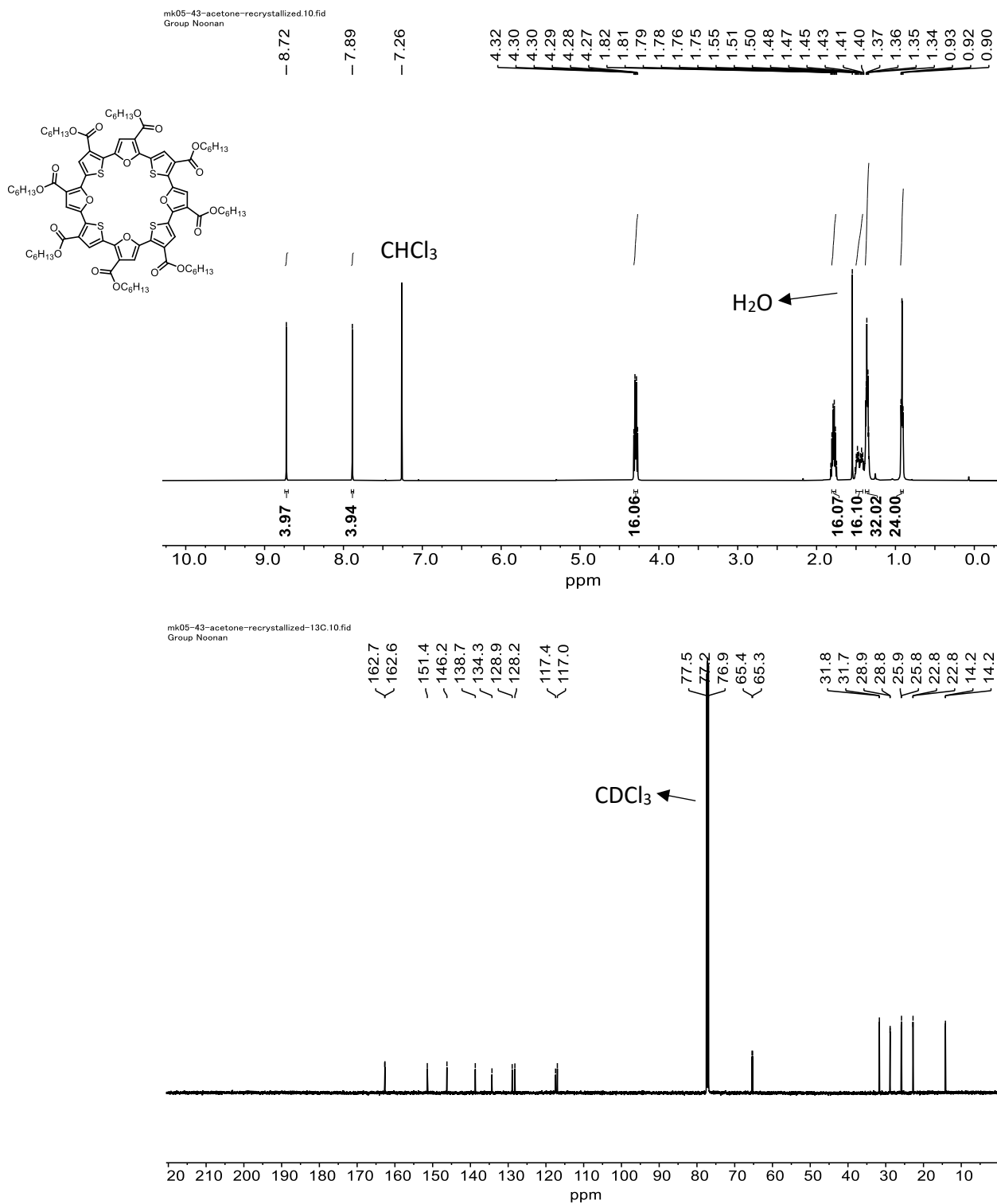


Figure S8. ¹H NMR spectrum (Top, 500 MHz, CDCl₃) and ¹³C NMR spectrum (Bottom, 126 MHz) of C4TE4FE collected in CDCl₃.

HRMS (ESI-MS or DART-MS)

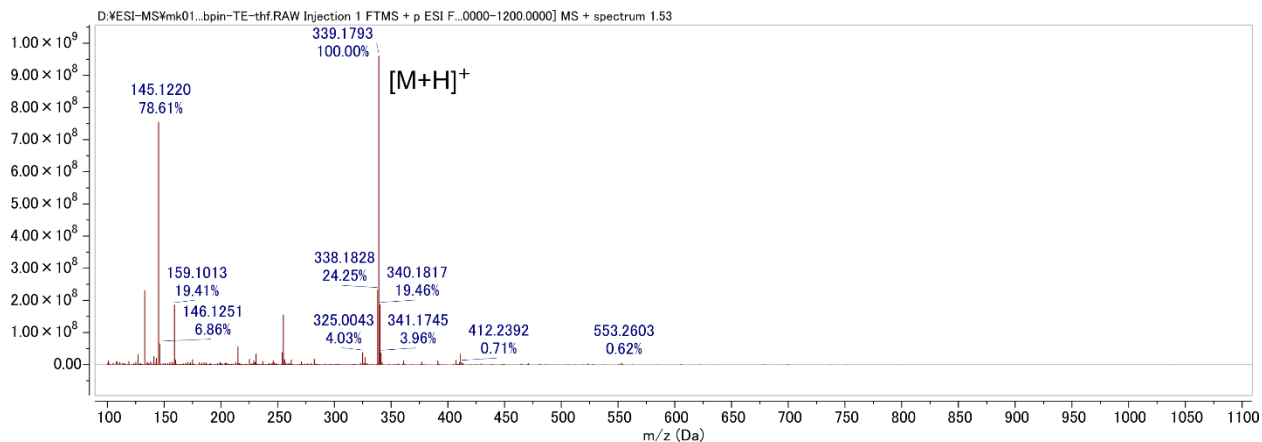


Figure S9. ESI-MS of hexyl 5-(4,4,5,5-tetramethyl-1,3,2-dioxaborolan-2-yl)thiophene-3-carboxylate.

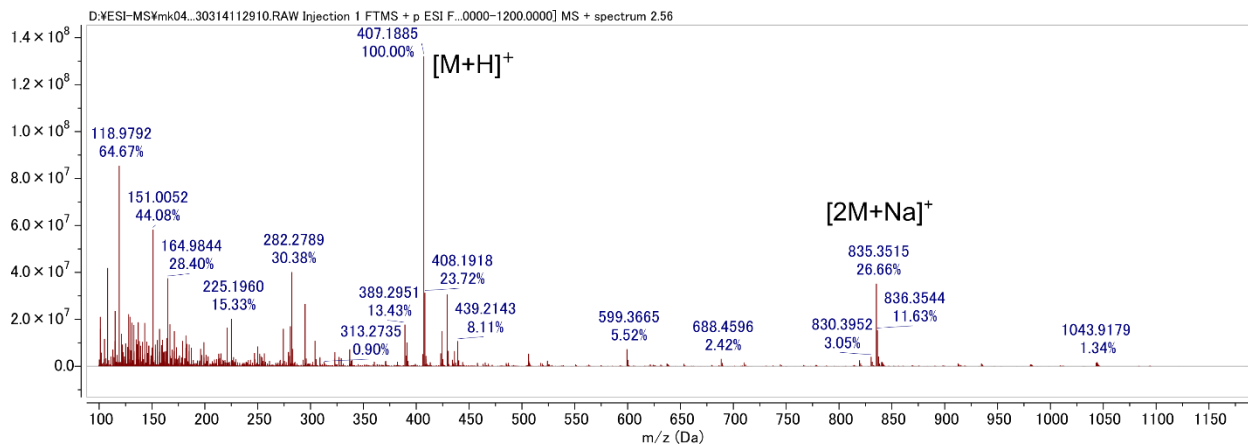


Figure S10. ESI-MS of FETE.

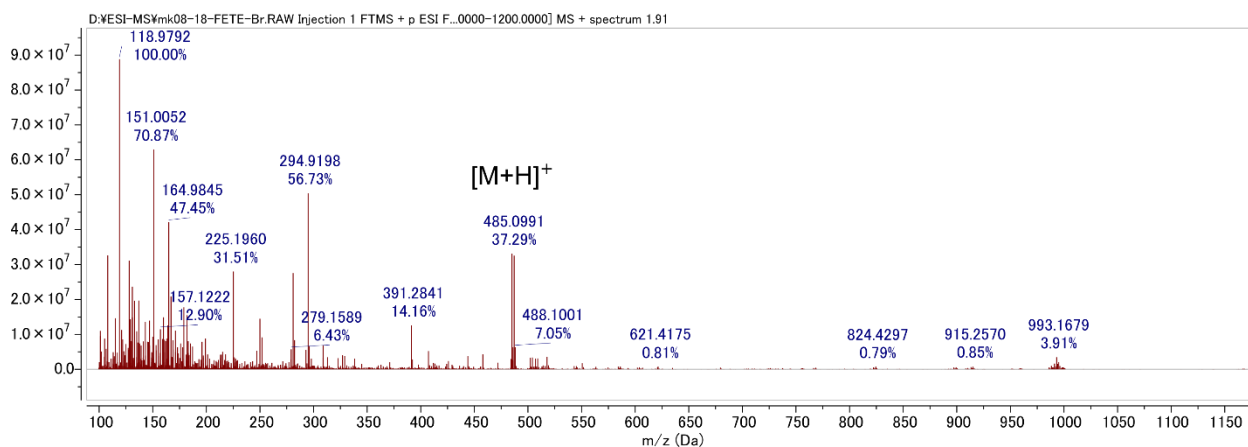


Figure S11. ESI-MS of FETE-Br

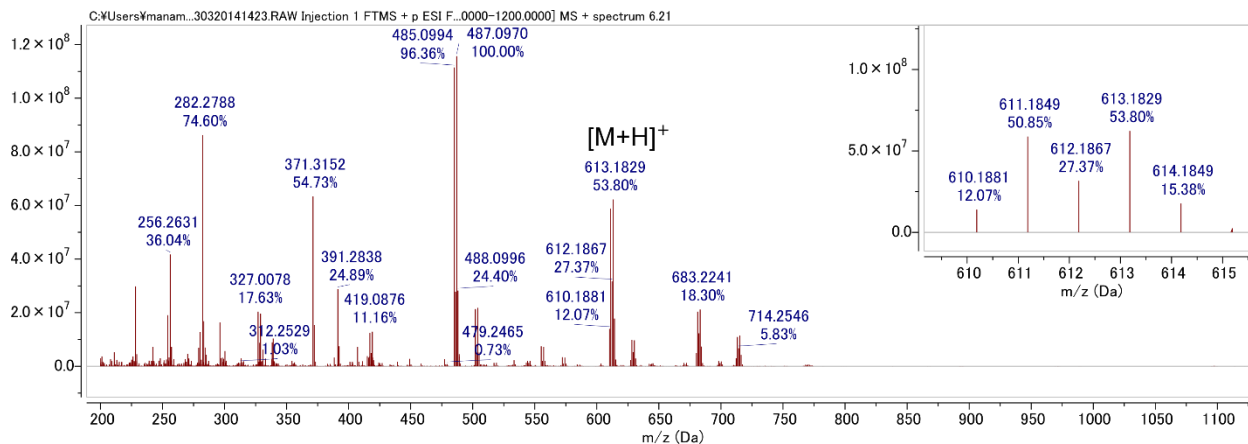


Figure S12. ESI-MS of Bpin-FETE-Br.

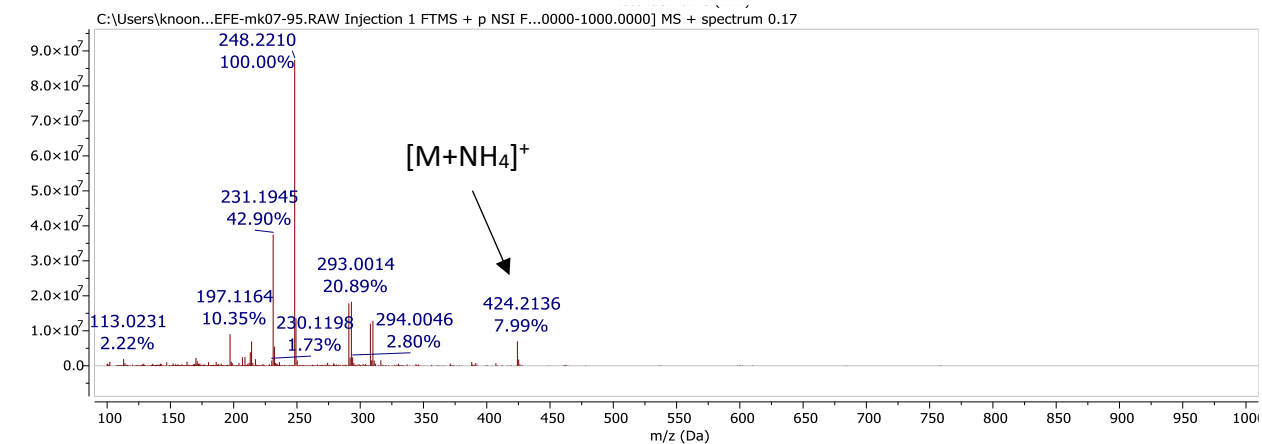


Figure S13. DART-MS of TEFE.

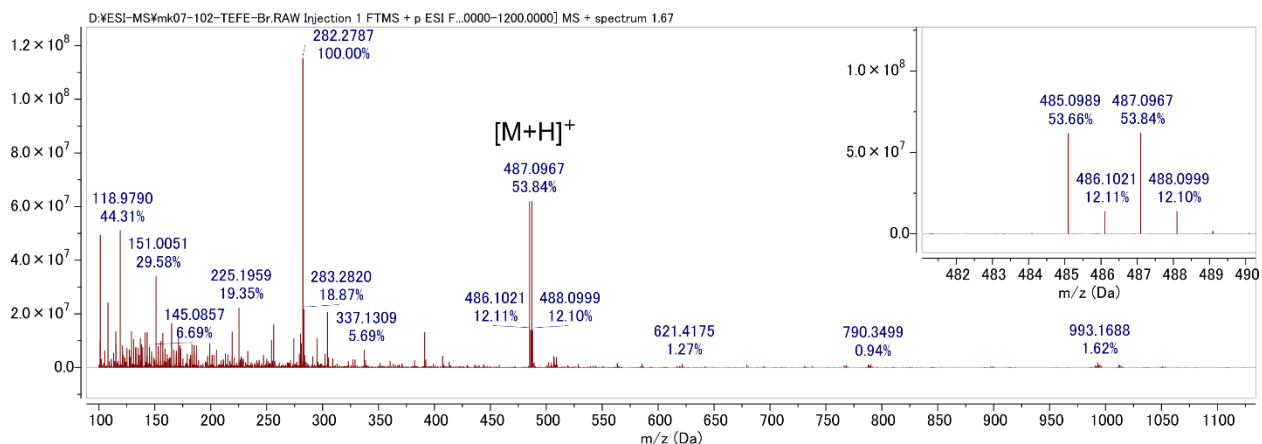


Figure S14. ESI-MS of TEFE-Br.

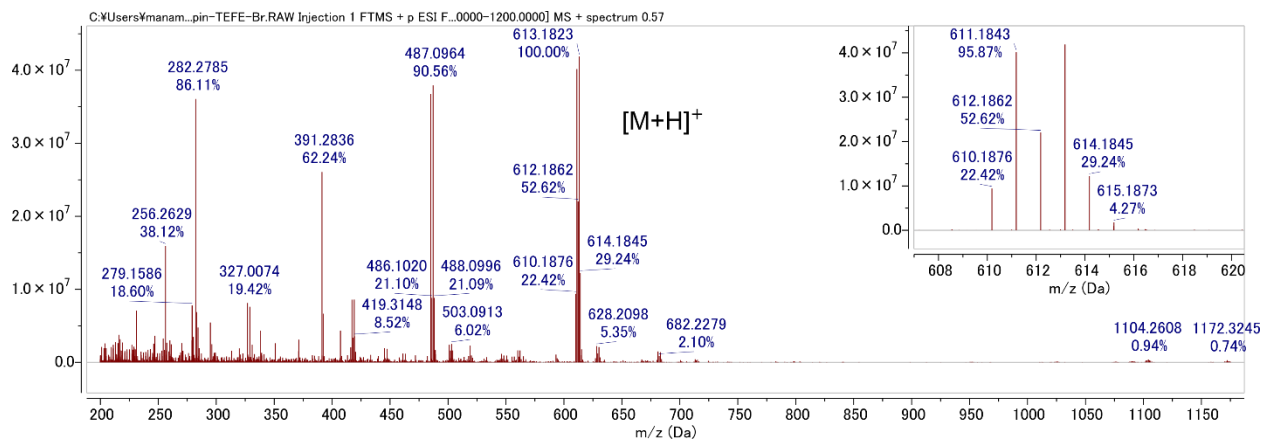


Figure S15. ESI-MS of **Bpin-TEFE-Br**.

FT-IR

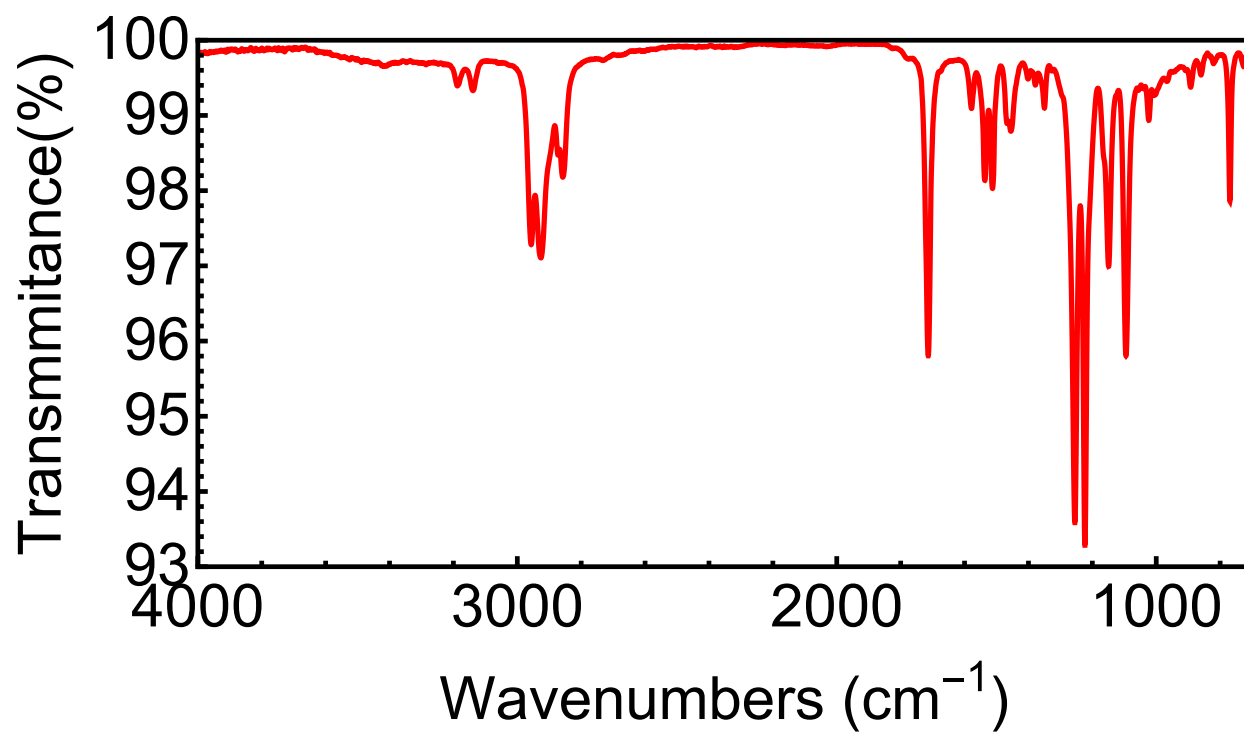


Figure S16. FTIR spectrum of C4TE4FE.

Determination of onset potentials on CV.

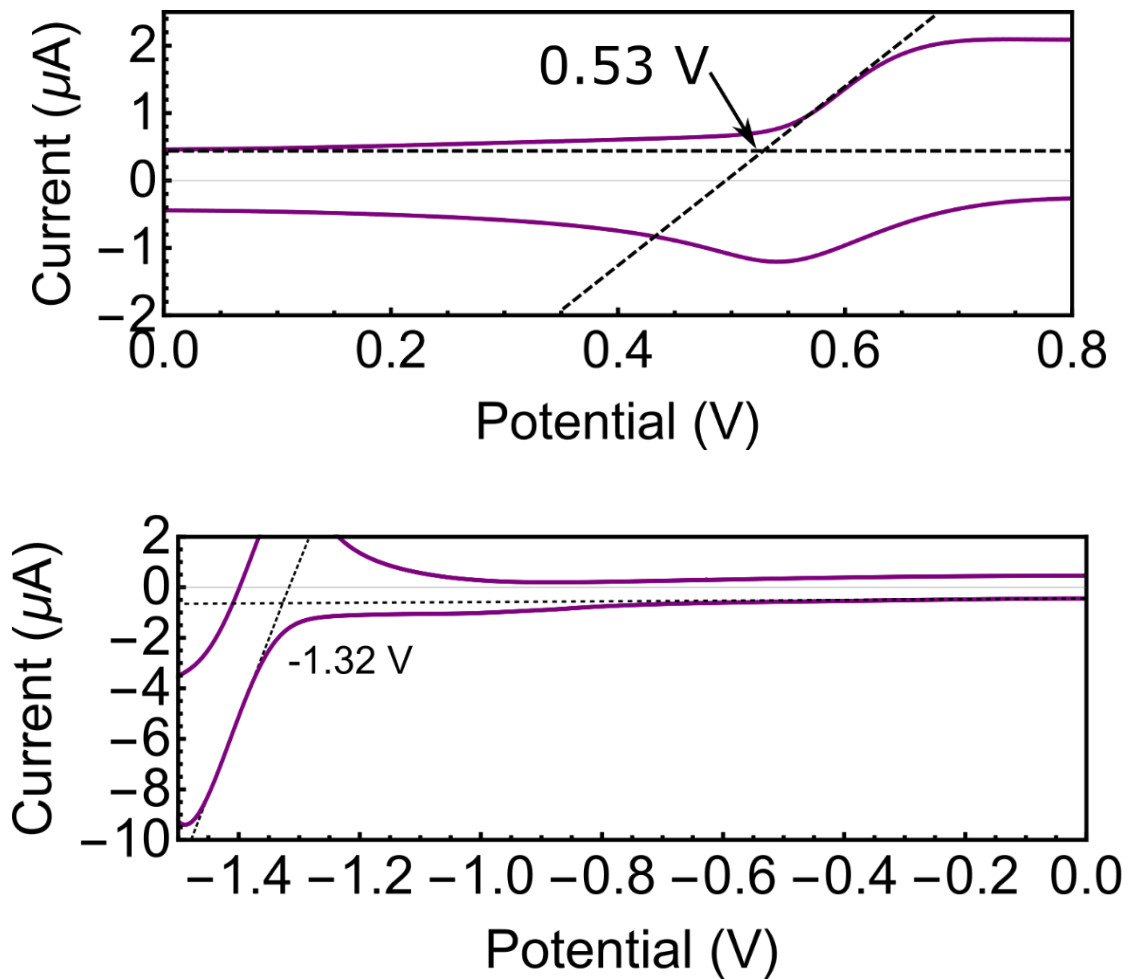


Figure S17. Determination of onset potentials for C4TE4FE in CH₂Cl₂.

Synthesis and isolation of $(C_4FE_4TE)^{2+} \cdot 2(SbCl_6^-)$

In a N_2 filled glovebox, a 20 mL scintillation vial was charged with C_4FE_4TE (3.4 mg, 2.10×10^{-3} mmol) in 1 mL of degassed CH_2Cl_2 (or CD_2Cl_2). To the reaction mixture, was added 0.2 mL of a $SbCl_5$ stock solution (10.0 mg/mL in CH_2Cl_2 or CD_2Cl_2) slowly using a syringe. The color of the solution immediately changed from brown to bright purple. After stirring for 5 min, the solvent was removed *in vacuo*. The resultant purple solid was washed with degassed hexane (3×1 mL) to give $(C_4FE_4TE)^{2+} \cdot 2(SbCl_6^-)$ as a purple solid (>99% yield). Signals listed below are from the crude reaction carried out in CD_2Cl_2 directly.

1H NMR (500 MHz, CD_2Cl_2) δ 14.55 (s, 4H), 13.66 (s, 4H), 5.55 (t, $J = 6.3$ Hz, 8H), 5.50 (t, $J = 6.6$ Hz, 8H), 2.70 – 2.56 (m, 16H), 2.24 (p, $J = 7.7$ Hz, 8H), 2.12 (p, $J = 7.6$ Hz, 8H), 1.90 – 1.78 (m, 16H), 1.78 – 1.65 (m, 16H), 1.19 (t, $J = 7.3$ Hz, 12H), 1.17 (t, $J = 7.3$ Hz, 12H).

^{13}C NMR (126 MHz, CD_2Cl_2) δ 165.5, 164.5, 150.1, 148.7, 147.3, 139.6, 136.7, 133.8, 132.1, 131.0, 69.3, 32.5, 32.4, 29.9, 29.8, 26.9, 26.7, 23.54, 23.46, 14.7, 14.6. The signal at 69.3 corresponds to an overlapping signal on both alkyl chains.

Attempted Synthesis of $C_6FE^{2+} \cdot 2(SbCl_6^-)$

In a N_2 filled glovebox, a 20 mL scintillation vial was charged with C_6FE (4.0 mg, 3.4×10^{-3} mmol) in 0.3 mL of CD_2Cl_2 . To the reaction mixture, was added 0.31 mL of a $SbCl_5$ stock solution (10.0 mg/mL in CD_2Cl_2) slowly using a syringe. The color of the solution immediately changed from red to green. After stirring for 5 min, the solvent was removed and the resultant green solid was washed with degassed hexane (3×1 mL). The isolated sample resulted in very broad NMR spectra and the spectra listed here are from the crude reaction mixture. Signals listed below are from the crude reaction carried out in CD_2Cl_2 directly.

1H NMR (500 MHz, CD_2Cl_2) δ 12.37 (s, 6H), 5.15 (t, $J = 6.6$ Hz, 12H), 2.35 (p, $J = 6.9$ Hz, 12H), 1.85 (p, $J = 7.7$ Hz, 12H), 1.69 – 1.61 (m, 12H), 1.60 – 1.50 (m, 12H), 1.07 (t, $J = 7.3$ Hz, 18H).

^{13}C NMR (126 MHz, CD_2Cl_2) δ 162.1, 146.1, 145.5, 137.3, 136.3, 69.5, 32.2, 29.4, 26.4, 23.3, 14.5.

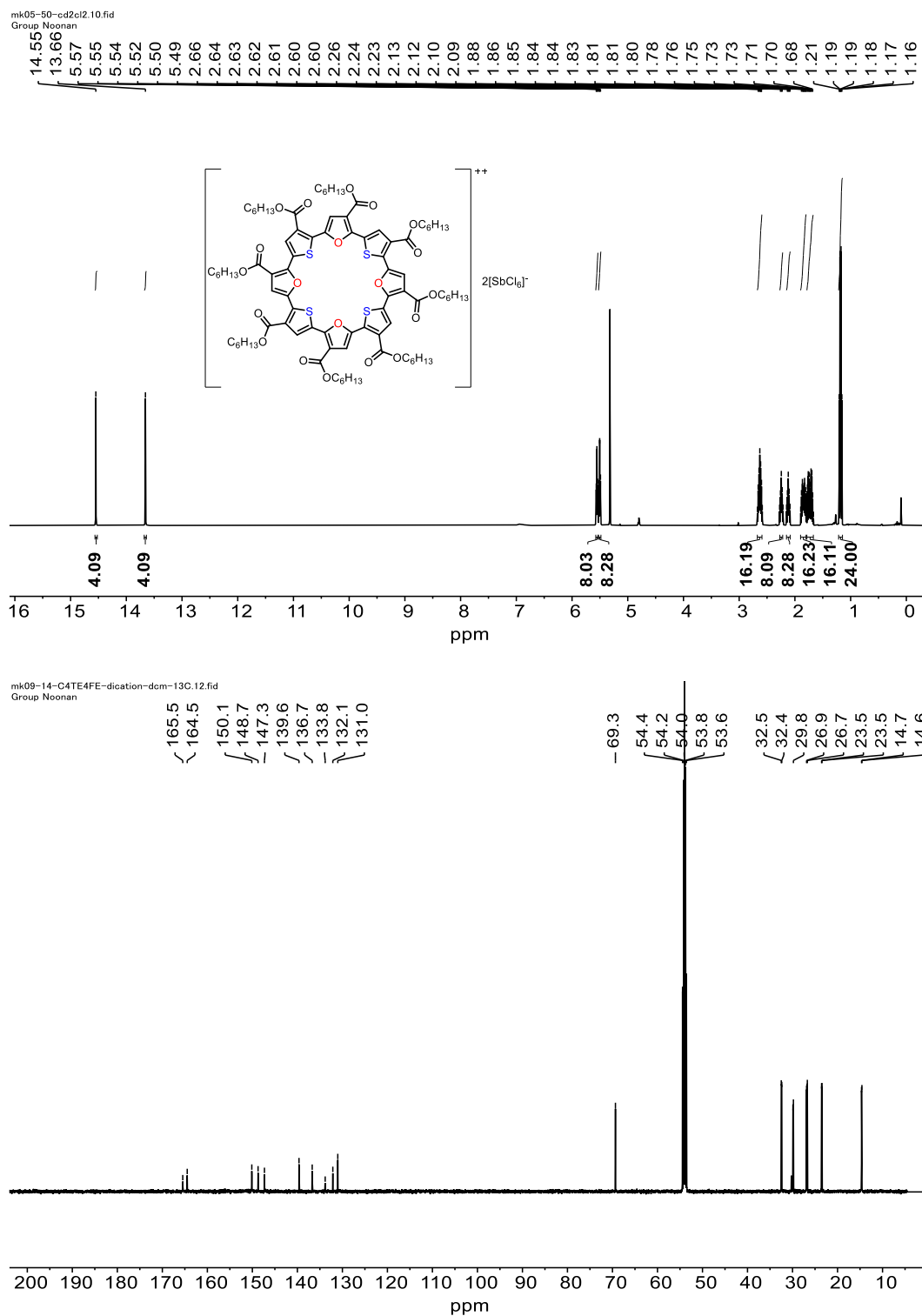


Figure S18. ^1H (Top) and ^{13}C (Bottom) NMR spectra of $(\text{C}_4\text{FE}_4\text{TE})^{2+} \cdot 2(\text{SbCl}_6)^-$ collected in CD_2Cl_2 at room temperature (500 and 126 MHz, respectively).

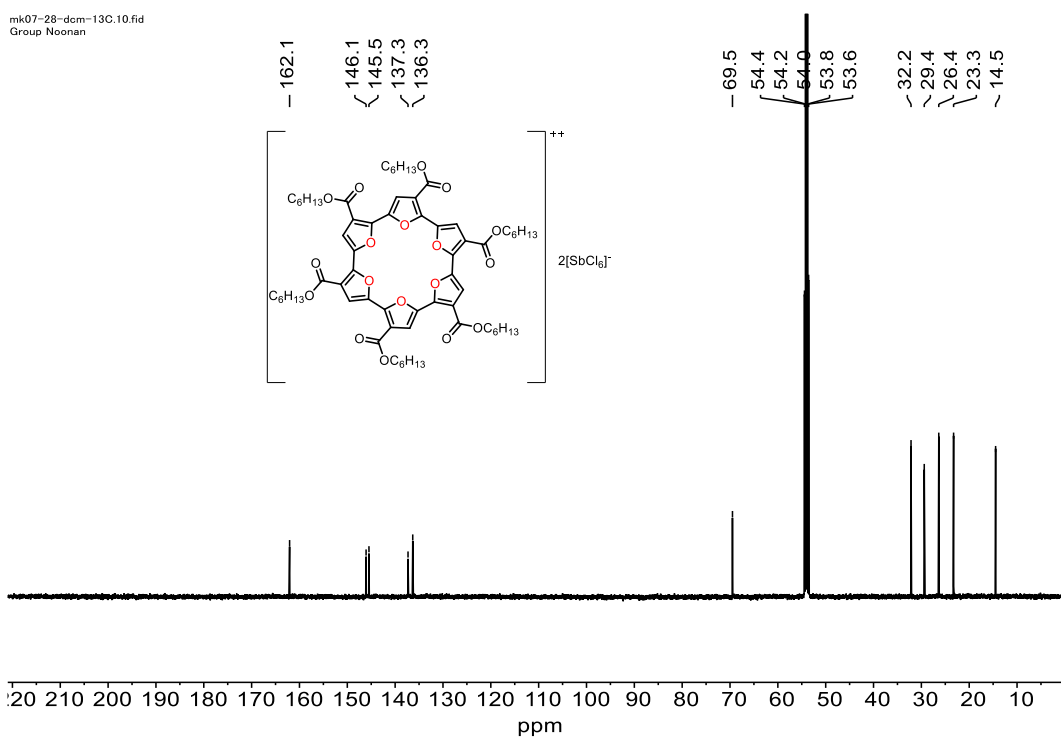
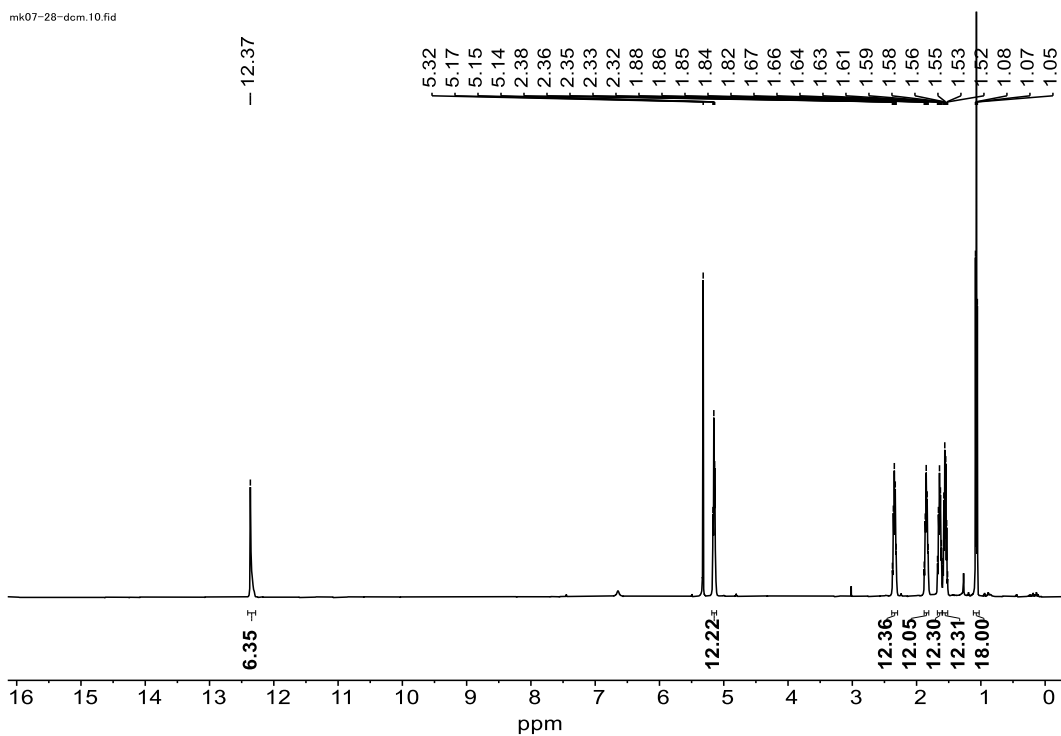


Figure S19. ^1H (Top) and ^{13}C (Bottom) NMR spectra of attempted synthesis of $(\text{C}_6\text{FE})^{2+\bullet} \cdot 2(\text{SbCl}_6^-)$ collected in CD_2Cl_2 at room temperature (500 and 126 MHz, respectively).

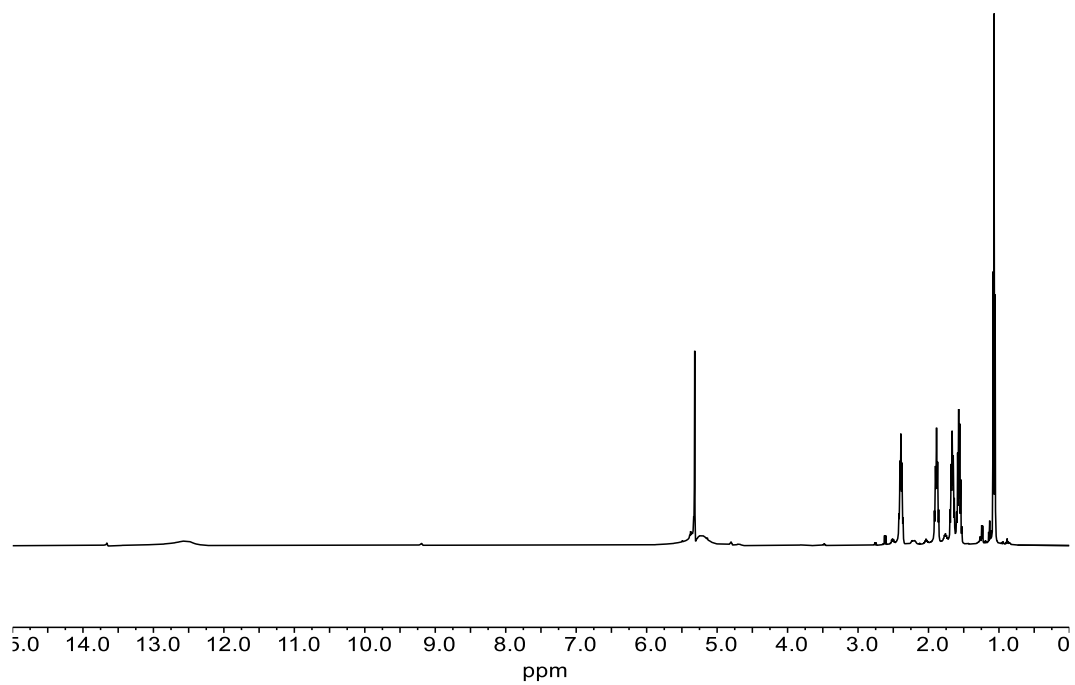


Figure S20. ¹H NMR spectrum (500 MHz, CD₂Cl₂) of **C₆FE²⁺•2(SbCl₆⁻)** after isolation.

EPR study for $(\text{C}_4\text{TE}_4\text{FE})^{2+} \cdot 2(\text{SbCl}_6^-)$

In a N_2 filled glovebox, a 20 mL scintillation vial was charged with $\text{C}_4\text{FE}_4\text{TE}$ (4.0 mg, 2.47×10^{-3} mmol) in ~ 0.8 mL of CD_2Cl_2 . To the reaction mixture, was added either 0.11 mL (1.5 equiv) or 0.3 mL (4 equiv) of a SbCl_5 stock solution (10.0 mg/mL in CD_2Cl_2). The color of the solution immediately changed from brown to dark brown with 1.5 equiv and to bright purple with 4 equiv. After stirring for 5 min, the solution was transferred to an EPR sample tube and frozen in liquid N_2 for EPR analysis. Solutions could also be transferred to an NMR tube for ^1H NMR analysis.

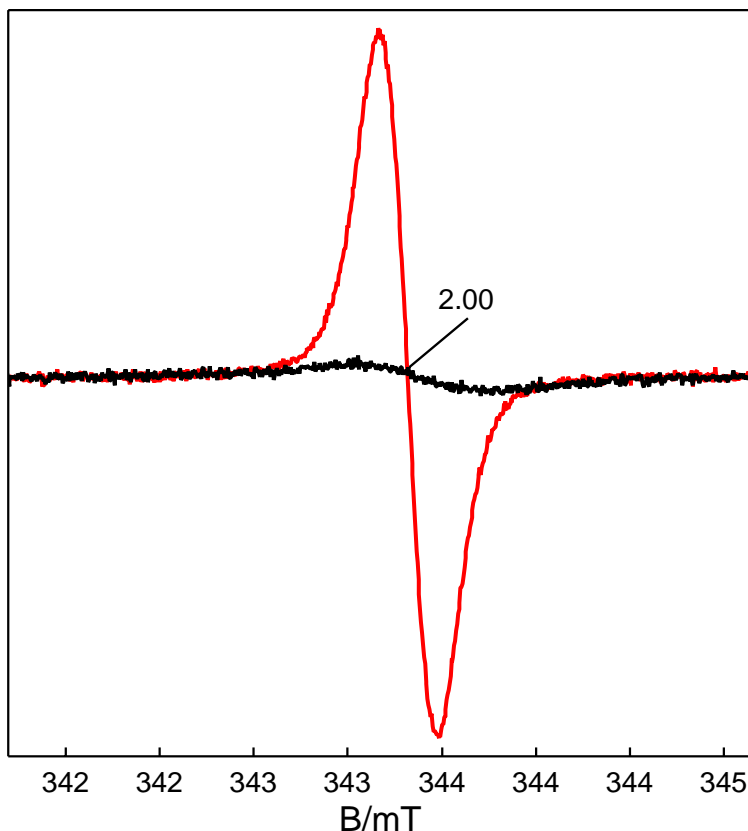


Figure S21. X-band EPR spectra of $\text{C}_4\text{TE}_4\text{FE}$ after combination with 1.5 equiv SbCl_5 (red) and 4 equiv of SbCl_5 (black). A clear radical signal at $g = 2$ with 0.04 mM in spin concentration was observed (total concentration of $\text{C}_4\text{TE}_4\text{FE}$ in solution is 2.7 mM). After addition of 4 equiv of SbCl_5 to $\text{C}_4\text{TE}_4\text{FE}$, the radical signal is present but at a very low concentration, < 0.004 mM (total concentration of macrocycle in solution is 2.2 mM). The measurement conditions: microwave frequency, 9.632 GHz, microwave power, $2 \mu\text{W}$, modulation amplitude, 1 Gauss, modulation frequency, 100 kHz, measurement temperature, 100 K.

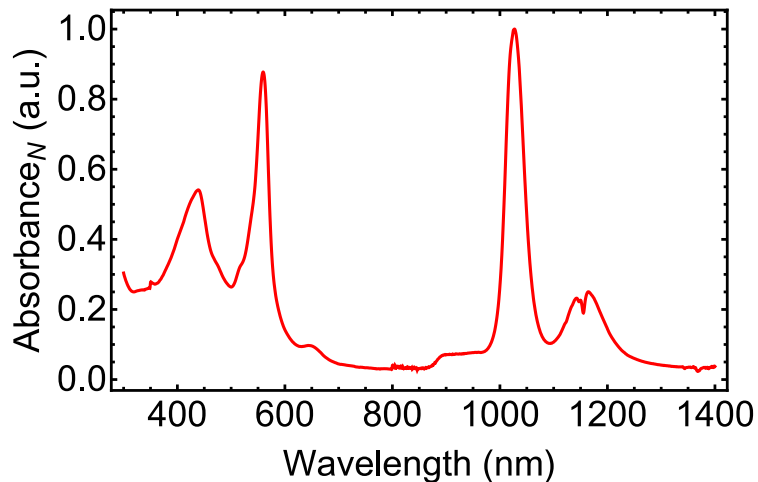


Figure S22. UV-Vis-NIR spectra of the isolated $[\text{C4TE4FE}]^{2+} \cdot 2\text{SbCl}_6^-$ in CH_2Cl_2 at room temperature preserved under nitrogen atmosphere for 1 month at $-40\text{ }^\circ\text{C}$.

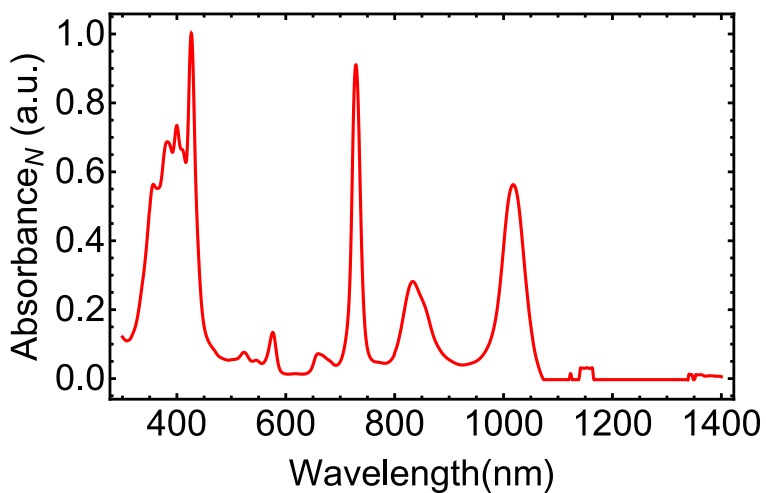


Figure S23. UV-Vis-NIR spectra of the $[\text{C6FE}]^{2+} \cdot 2\text{SbCl}_6^-$ in CH_2Cl_2 at room temperature after attempting the isolation.

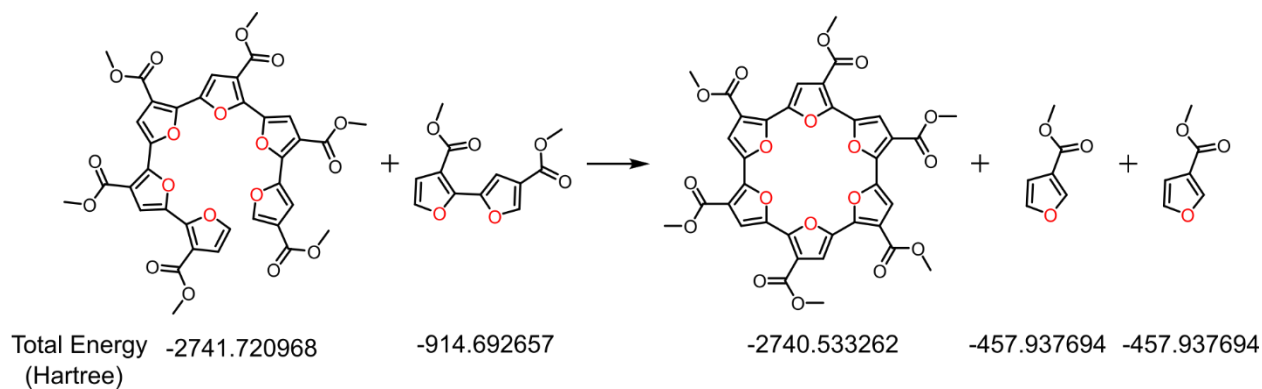


Figure S24. Ring strain energy calculation for *me*-C6FE which was computed by taking the difference in total energies for the products and reactants shown above ($E_{\text{prod}} - E_{\text{react}}$). Calculations for all structures were carried out at the B3LYP-D3(BJ)/6-31G(d,p) level, with a IEFPCM solvation model using CH_2Cl_2 as the solvent. The total energy difference (which also corresponds to the enthalpy of formation in this instance) then serves as the ring strain energy for *me*-C6FE which is **3.1 kcal/mol** in this case.

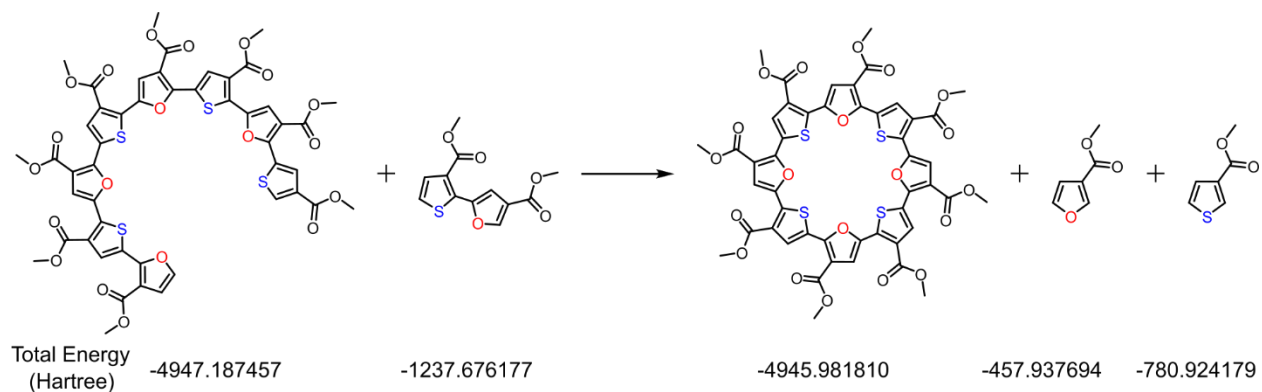


Figure S25. Ring strain energy calculation for *me*-C4TE4FE computed by taking the difference in total energies for the products and reactants shown above ($E_{\text{prod}} - E_{\text{react}}$). Calculations for all structures were carried out at the B3LYP-D3(BJ)/6-31G(d,p) level, with a IEFPCM solvation model using CH_2Cl_2 as the solvent. The total energy difference (which also corresponds to the enthalpy of formation in this instance) then serves as the ring strain energy for *me*-C4TE4FE which is **12.5 kcal/mol** in this case.

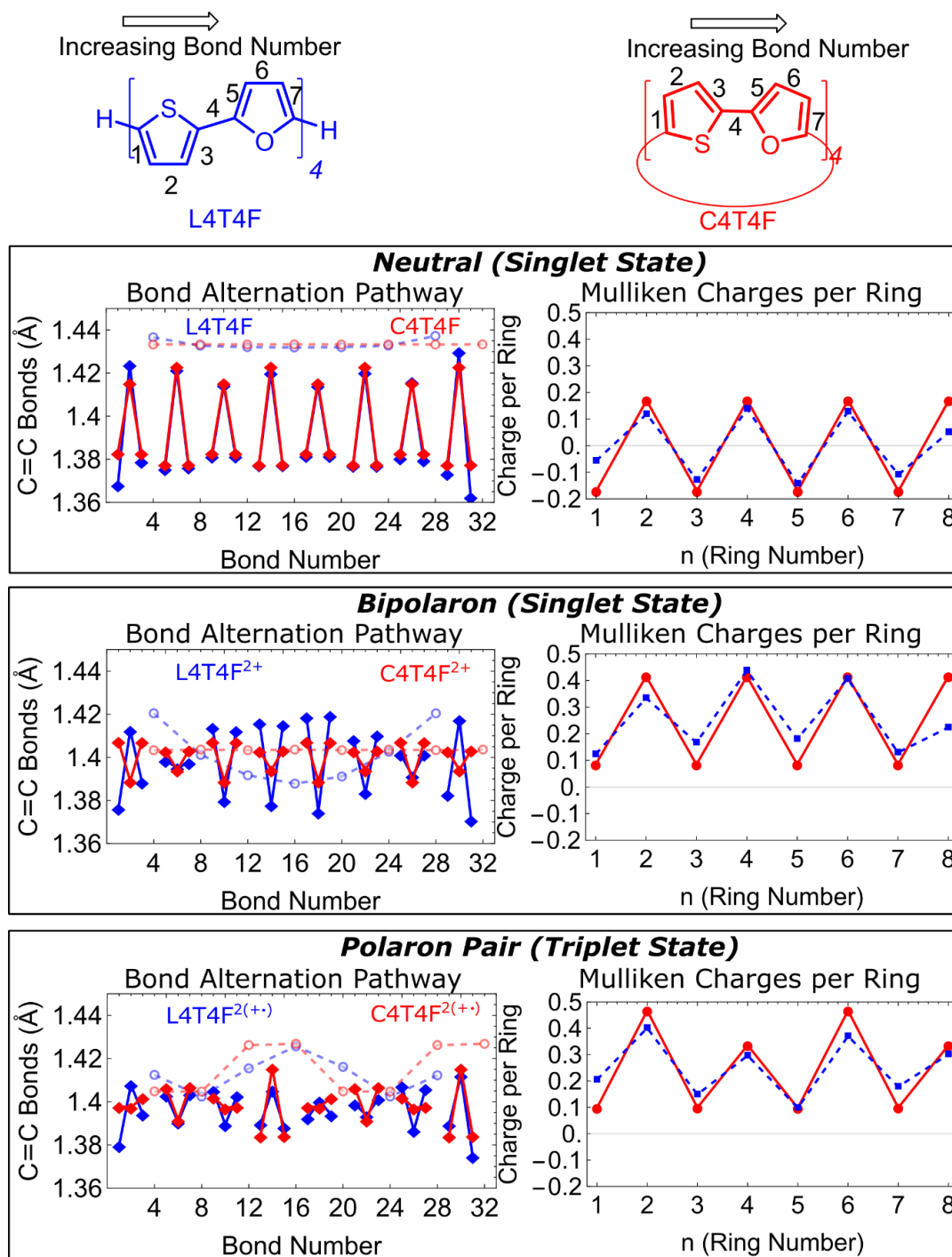


Figure S26. Bond alternation pathway (left) and Mulliken charge distribution per ring (right) calculated for a linear and cyclic alternating thiophene-furan oligomer at the B3LYP-D3(BJ)/6-31G(d,p) level, with a IEFPCM solvation model using CH_2Cl_2 as the solvent. The open circles in the bond alternation pathway plots correspond to the interring bonds in each case.

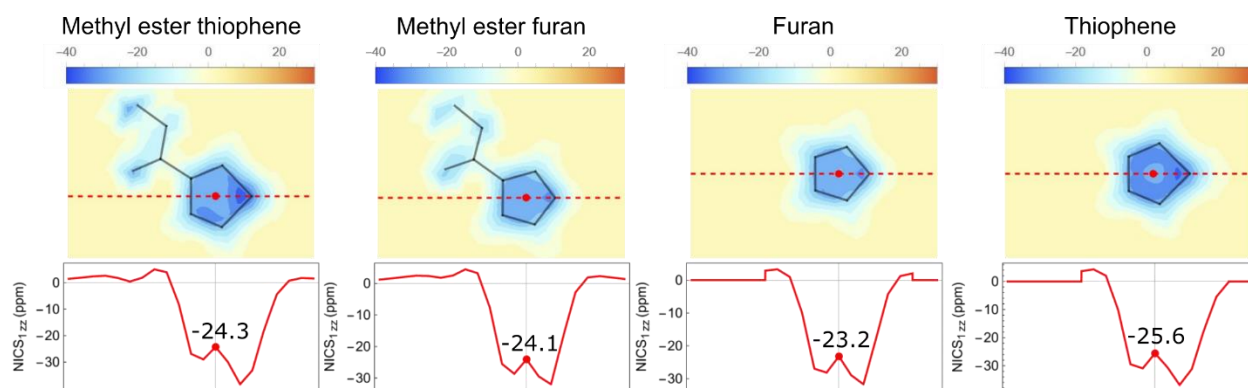


Figure S27. NICS(1)_{zz} calculations with color maps to illustrate diatropic (blue) or paratropic (brown to red) ring current for methyl thiophene-3-carboxylate and methyl furan-3-carboxylate along with furan and thiophene. The line plots at the bottom shows the NICS value profile along the line(dashed red) passing through the center of the heterocycle.

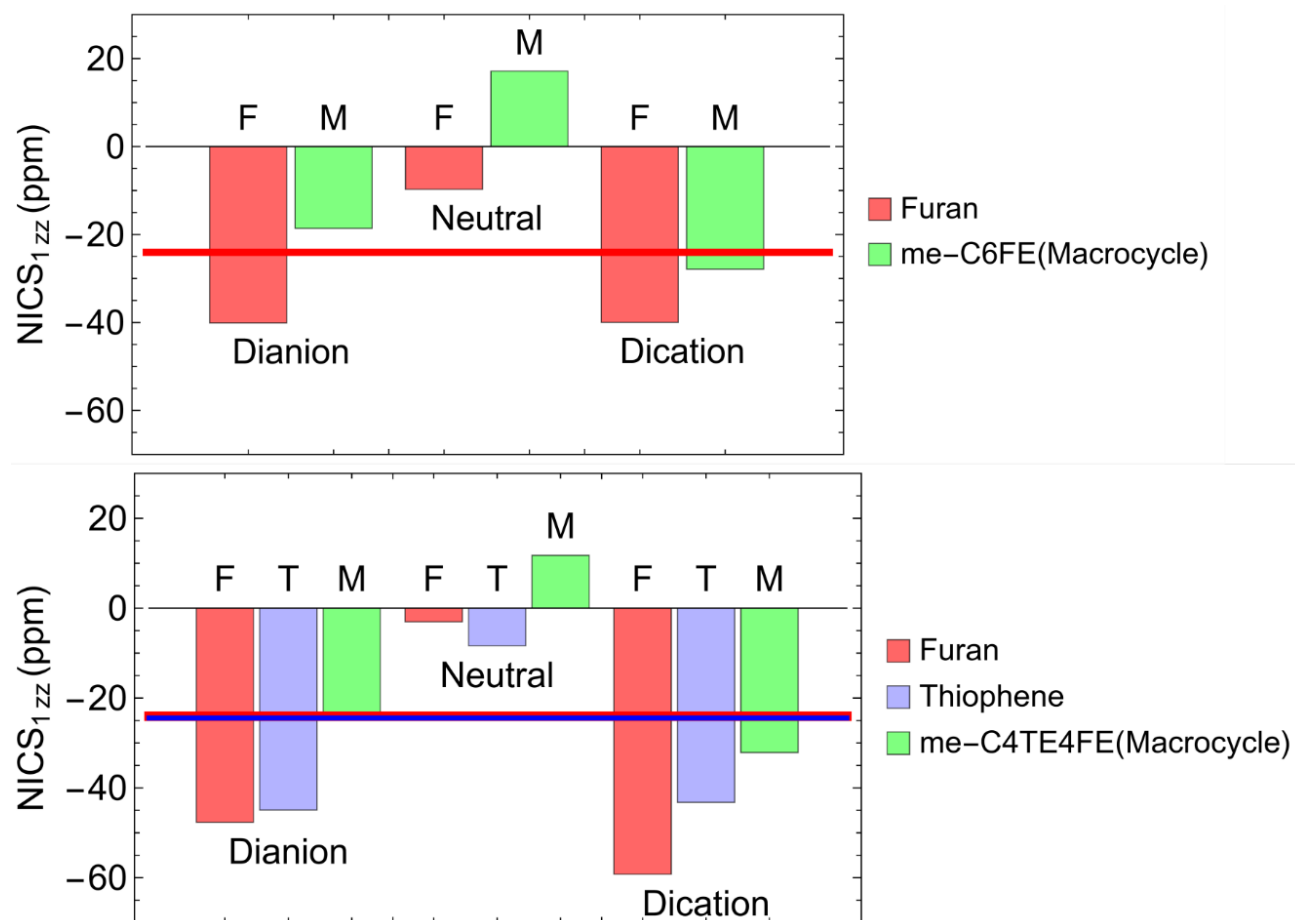


Figure S28. Bar charts illustrating the NICS(1)_{zz} value for the *me-C6FE* (top) and *me-C4TE4FE* (bottom). In each plot, the NICS values at the center of the individual heterocycle and entire macrocycle are noted for the relevant redox states (dianion, neutral and dication forms). Horizontal lines correspond to the NICS values to the parent methyl thiophene-3-carboxylate(blue) and methyl furan-3-carboxylate(red).

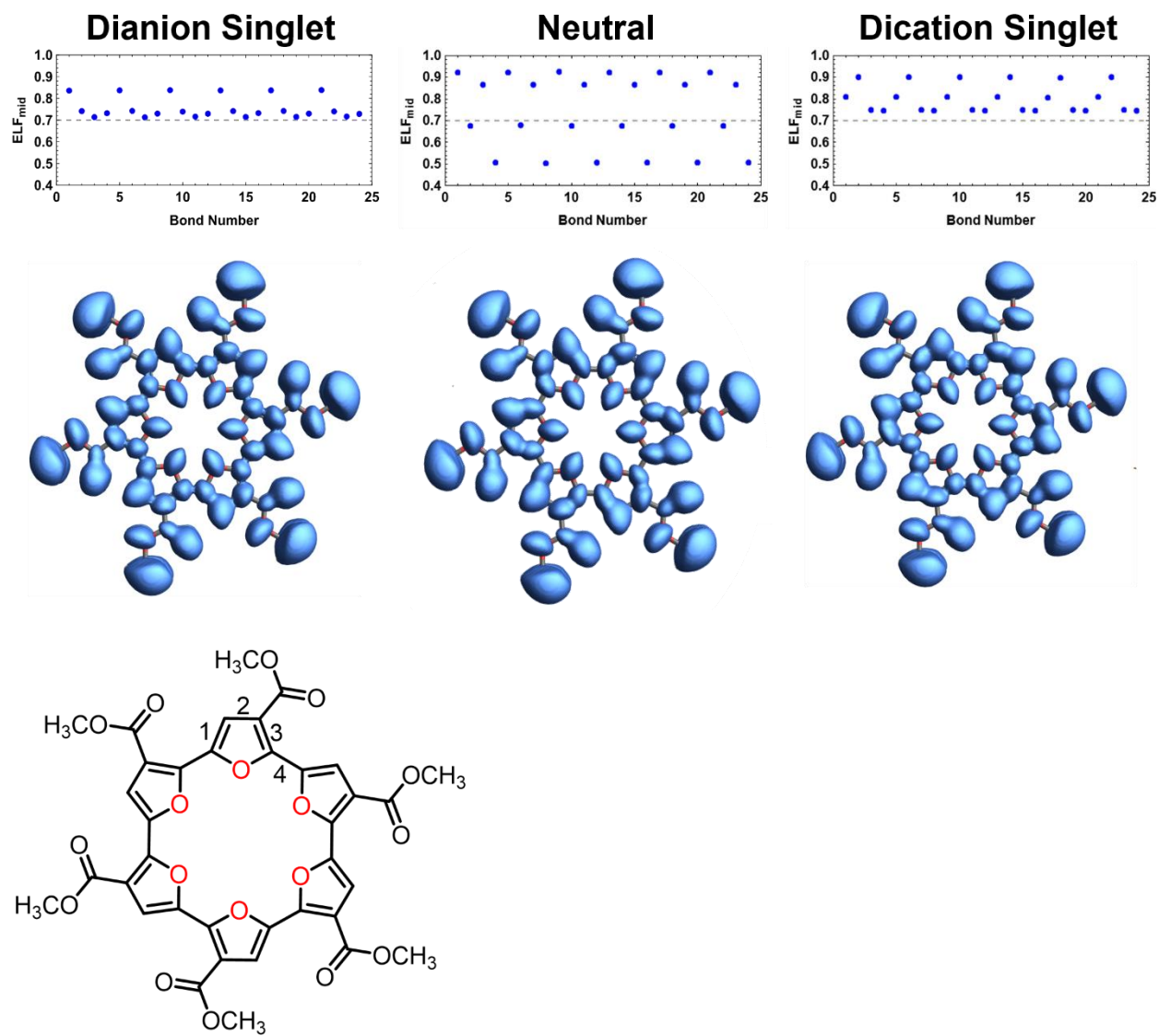


Figure S29: ELF plots for the *me*-C6FE dianion singlet(left), neutral(middle), and dication singlet(right) plotted with isosurface values of 0.7. Bonds 1 through 4 are labelled and the numbers continue around the macrocycle (24 total bonds). Interring bonds are 4, 8, 12, 16, 20, 24.

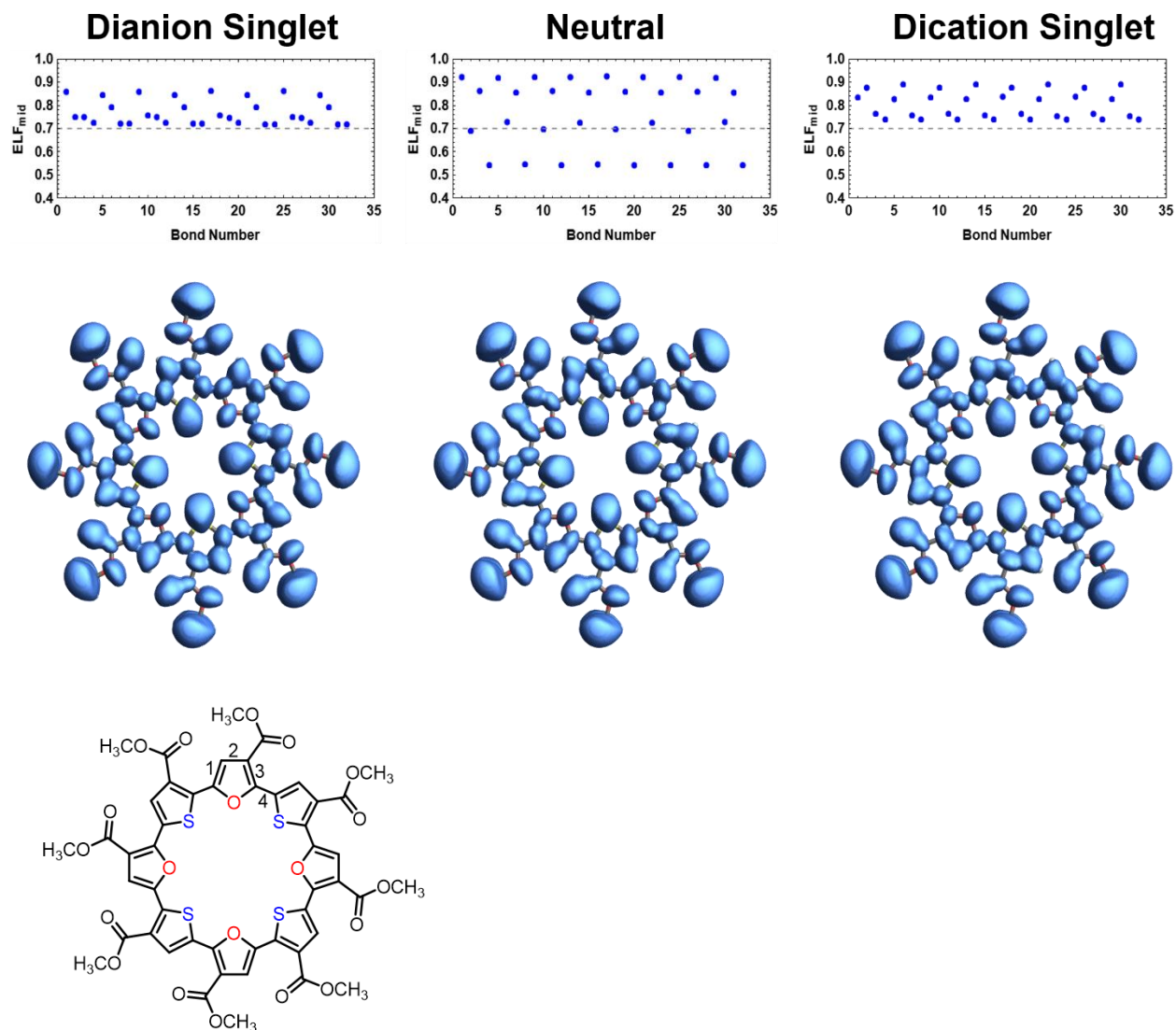


Figure S30: ELF plots for the *me*-C₄TE₄FE dianion singlet(left), neutral(middle), and dication singlet(right) plotted with isosurface values of 0.7. Bonds 1 through 4 are labelled and the numbers continue around the macrocycle (32 total bonds). Interring bonds are 4, 8, 12, 16, 20, 24, 28, 32.

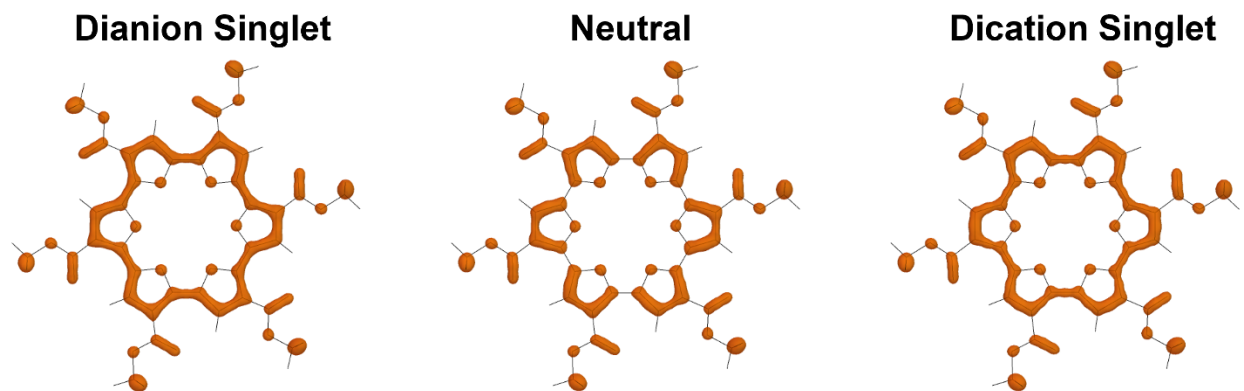


Figure S31. Localized-orbital locator (LOL) plots of *me-C6FE*.

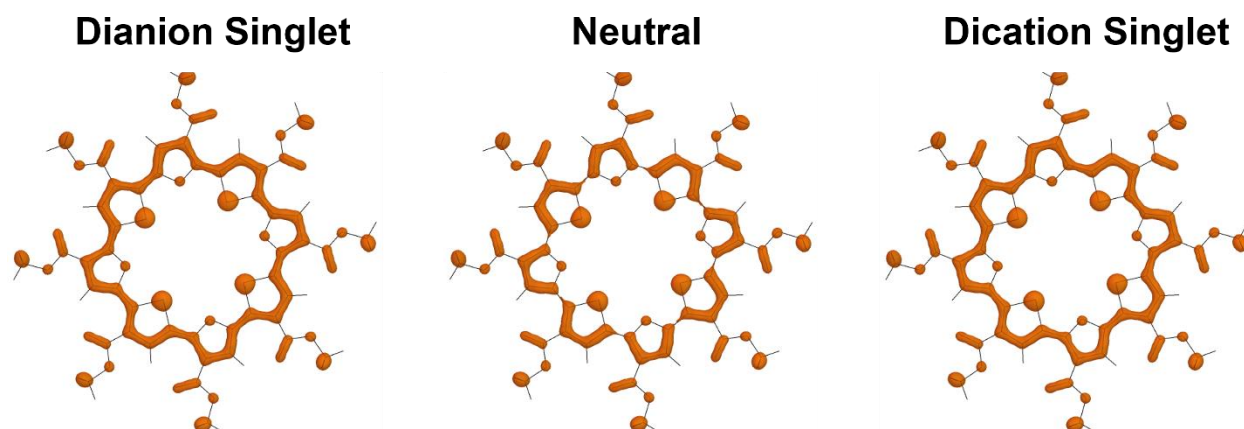


Figure S32. Localized-orbital locator (LOL) plots of *me-C4TE4FE*.

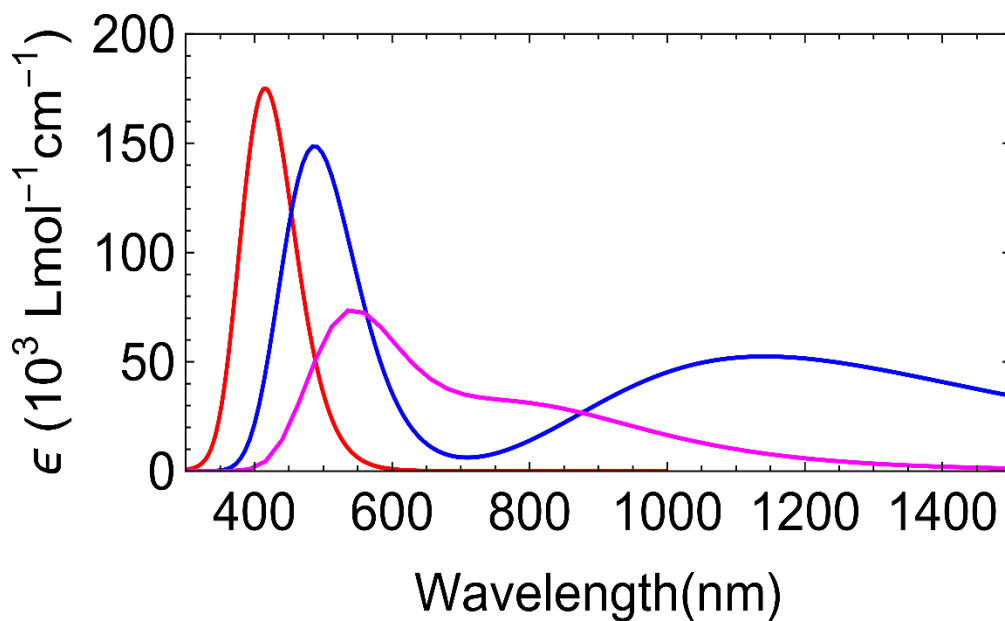


Figure S33. TD-DFT predicted absorbance spectra for *me*-C4TE4FE (red), *me*-C4TE4FE²⁺ (blue), and *me*-C4TE4FE^{2•+} (magenta). Calculations were performed at CAM-B3LYP/6-31G(d,p) IEFPCM(CH₂Cl₂) level.

Table S1. Shielding Tensors and Computed Chemical Shifts for *me*-C6FE and *me*-C4TE4FE as well as the oxidized forms. Calculations for both the macrocycles were carried out using B3LYP-D3(BJ) and ω B97XD functionals and 6-31G(d,p) basis sets with a IEFPCM solvation model using CH₂Cl₂ as the solvent.

$$\text{TMS(B3LYP-D3(BJ))} = 32.4256$$

$$\text{TMS}(\omega\text{B97xD}) = 32.4335$$

	Shielding Constant (B3LYP-D3(BJ))	Chemical Shift	Shielding Constant (ω B97xD)	Chemical Shift
<i>me</i>-C6FE				
Aromatic Signal	23.96	8.47	23.92	8.51
Methyl Ester	27.92	4.51	27.96	4.47
<i>me</i>-C6FE²⁺				
Aromatic Signal	18.61	13.81	18.20	14.23
Methyl Ester	26.81	5.62	26.77	5.66
<i>me</i>-C4TE4FE				
Th Aromatic Signal	22.36	10.06	21.47	10.96
Fu Aromatic Signal	22.91	9.52	22.15	10.28
Th Methyl Ester	27.85	4.57	27.73	4.71
Fu Methyl Ester	27.84	4.59	27.74	4.70
<i>me</i>-C4TE4FE²⁺				
Th Aromatic Signal	14.75	17.67	14.81	17.62
Fu Aromatic Signal	15.77	16.66	15.78	16.65
Th Methyl Ester	26.14	6.28	26.31	6.12
Fu Methyl Ester	26.19	6.23	26.36	6.07

References

- [1] A. J. Varni, M. Kawakami, S. A. Tristram-Nagle, D. Yaron, T. Kowalewski, K. J. T. Noonan, *Org. Chem. Front.* **2021**, *8*, 1775-1782.
- [2] Y. Qiu, J. C. Worch, A. Fortney, C. Gayathri, R. R. Gil, K. J. T. Noonan, *Macromolecules* **2016**, *49*, 4757-4762.
- [3] D. T. Petasis, M. P. Hendrich, in *Methods in Enzymology, Vol. 563* (Eds.: P. Z. Qin, K. Warncke), Academic Press, **2015**, pp. 171-208.
- [4] M. J. Frisch, G. W. Trucks, H. B. Schlegel, G. E. Scuseria, M. A. Robb, J. R. Cheeseman, G. Scalmani, V. Barone, G. A. Petersson, H. Nakatsuji, X. Li, M. Caricato, A. V. Marenich, J. Bloino, B. G. Janesko, R. Gomperts, B. Mennucci, H. P. Hratchian, J. V. Ortiz, A. F. Izmaylov, J. L. Sonnenberg, Williams, F. Ding, F. Lipparini, F. Egidi, J. Goings, B. Peng, A. Petrone, T. Henderson, D. Ranasinghe, V. G. Zakrzewski, J. Gao, N. Rega, G. Zheng, W. Liang, M. Hada, M. Ehara, K. Toyota, R. Fukuda, J. Hasegawa, M. Ishida, T. Nakajima, Y. Honda, O. Kitao, H. Nakai, T. Vreven, K. Throssell, J. A. Montgomery Jr., J. E. Peralta, F. Ogliaro, M. J. Bearpark, J. J. Heyd, E. N. Brothers, K. N. Kudin, V. N. Staroverov, T. A. Keith, R. Kobayashi, J. Normand, K. Raghavachari, A. P. Rendell, J. C. Burant, S. S. Iyengar, J. Tomasi, M. Cossi, J. M. Millam, M. Klene, C. Adamo, R. Cammi, J. W. Ochterski, R. L. Martin, K. Morokuma, O. Farkas, J. B. Foresman, D. J. Fox, Wallingford, CT, **2016**.
- [5] a) H. L. Schmider, A. D. Becke, *J. Mol. Struct. THEOCHEM* **2000**, *527*, 51-61; b) H. L. Schmider, A. D. Becke, *J. Chem. Phys.* **2002**, *116*, 3184-3193.
- [6] A. D. Becke, K. E. Edgecombe, *J. Chem. Phys.* **1990**, *92*, 5397-5403.
- [7] a) T. Lu, F.-W. Chen, *Acta Phys. -Chim. Sin.* **2011**, *27*, 2786-2792; b) T. Lu, F. W. Chen, *J. Comput. Chem.* **2012**, *33*, 580-592.